ER-4571

AN INTEGRATED INTERPRETATION OF AEROMAGNETIC DATA IN THE PALEOZOIC OF THE NEBRASKA PANHANDLE

by

Joseph P. Fagan, Jr.

ER-4571

A thesis submitted to the Faculty and the Board of Trustees of the Colorado School of Mines in partial fulfillment of the requirements for the degree of Master of Engineering (Geophysical Engineer).

Golden, Colorado

Date 4/1/96

Signed: _____
Joseph P. Fagan, Jr.

Approved: _____
Dr. Gary Olhoeft
Thesis Advisor

Golden, Colorado

Date 3 April 1996

_____
Dr. Phillip R. Romig, Head
Department of Geophysics

ABSTRACT

The manual interpretation of aeromagnetic data can be a time consuming and labor intensive process. Because of the non-uniqueness of potential field geophysics, the analysis of a geophysical dataset can be influenced by the amount of experience the engineer has in a geologic setting. Also, if the engineer possesses geologic misconceptions about a basin, this will hinder, if not prevent, the successful interpretation of data.

This study in the Nebraska Panhandle seeks to combine a thorough understanding of subsurface geology with a high-quality aeromagnetic dataset to generate an interpretation that explains the locations of hydrocarbon emplacement. Also, the conventional interpretation is compared with an automated interpretation utilizing a conventional back propagation neural network. The two interpretations yield similar interpretation results that correlate very well with known production. The automated interpretation also locates several unexplored areas, based upon aeromagnetic data, that should be structurally higher and, therefore, possible hydrocarbon traps.

TABLE OF CONTENTS

LIST OF FIGURES

LIST OF TABLES

ACKNOWLEDGEMENTS

The author wishes to express his gratitude to a number of friends, both professional and personal. From the Colorado School of Mines, he thanks Dr. Abdelwahid Ibrahim for his encouragement to pursue a project outside of the department and for all of his support while completing the necessary coursework. Also, he thanks the members of his committee who, for many months, have given their support and patiently waited for the completion of this manuscript. He is greatly indebted to Mr. John Webb, consulting geologist, for the amount of advice and information he provided on the geology of Nebraska. He thanks Mr. John Schmunk of Airmag Surveys, Inc. who acquired, partly owns, and allowed the showing of the aeromagnetic survey for this report. The author acknowledges all of his instructors and former co-workers at the University of Illinois and Illinois State Geologic Survey. Lastly, the author owes Pearson, deRidder and Johnson most sincere thanks. Eduard deRidder and Robert Johnson have provided this dataset, critical review of this research, and overwhelming support on this and many other projects.

The author expresses his gratitude and love for his parents who have encouraged him for as long as he can remember, his soon-to-be-wife Jeanne Marie who has stood beside him throughout everything, and most of all, God---without His continuous support I could not succeed, but with His support, I could not fail.

INTRODUCTION

Magnetic prospecting is the oldest form of geophysical exploration (Dobrin and Savit, 1988). Magnetics have been used extensively to solve problems in a variety of areas, but especially in mineral prospecting, engineering studies, and oil and gas exploration. Although the primary geophysical tool in oil and gas exploration is reflection seismology, potential field geophysics, especially aeromagnetic prospecting, is an attractive option for several reasons. First, potential fields yield information about the total basin. That is, the magnetic response over an area is the summation of all of the sources below. This facilitates the interpretation of features which, in some basins, are too deep to produce a measurable seismic response. Secondly, the acquisition of potential field data is much easier than for seismic data. As both airborne magnetic and gravity studies are now common, these data are much easier to acquire in rugged and less accessible terrains. Thirdly, and perhaps most important in exploration, the cost of acquiring aeromagnetic data is a small fraction of that for seismic data. Thus, a high quality potential field database can greatly improve a petroleum exploration program at low cost.

There are drawbacks to potential field analyses. Guo (1992) lists several of these, including: (1) the difficulty of data analysis, (2) the inversion problem, or non-uniqueness, of defining a causative body, and (3) the potential for different interpretations. Seismic data

interpretation is in many cases much more straightforward and than for potential fields. While there are many software packages to aid in seismic processing and interpretation, the automation of potential field studies has lagged.

Nevertheless, potential field geophysics, especially magnetics, has an important role in exploration (Nettleton, 1976). As an example, a high-resolution aeromagnetic survey was acquired in the northeastern Denver-Julesberg Basin. The survey covers an area of 56 townships in the southwestern Nebraska Panhandle and northeastern Colorado (Figure 1). Within the survey area, there is extensive petroleum production from the Lower Cretaceous "D" and "J" sands. Drilling was later extended downward into the subjacent Permo-Pennsylvanian sediments with a resultant discovery at Amazon Field in Cheyenne County, Nebraska. At present, this field has a cummulative recovery of 223,000 barrels of oil. Because of the relatively shallow depths to these productive horizons, additional drilling has continued. Within the latter half of the 1980's several fields were discovered. These include Bird, Anna, Mathewson, Kleinholtz, and Terrestrial-Dill fields (Figure 1). Each of the fields that have been discovered to date are productive from a combination of structural-stratigraphic traps. Table 1 lists the amounts of production from these fields. High-resolution magnetic data that have been carefully processed and integrated with known geology can yield not only reconnaissance information for additional geophysical surveys, but also can stand alone as an exploration program.

The purposes of this integrated interpretation, then, are threefold. First, this report

Field	Oil production (barrels)	Gas production (MMCFG)	Water production (barrels)
Amazon	223,300	2,200	1,609,700
Anna	193,700	15,100	17,900
Bird	1,538,000	4,800	6,365,000
Dill	31,100	0	0
Kleinholz	2,495,300	1,211,500	160,800
Mathewson	155,700	10,500	548,800
Swearingen	99,800	182,800	55,000
Terrestrial	350,400	85,100	158,500

Table 1. Summary of Paleozoic oil and gas production from parts of Kimball County and Cheyenne County, Nebraska (pers. comm., Nebraska Oil and Gas Commision, 1/96)

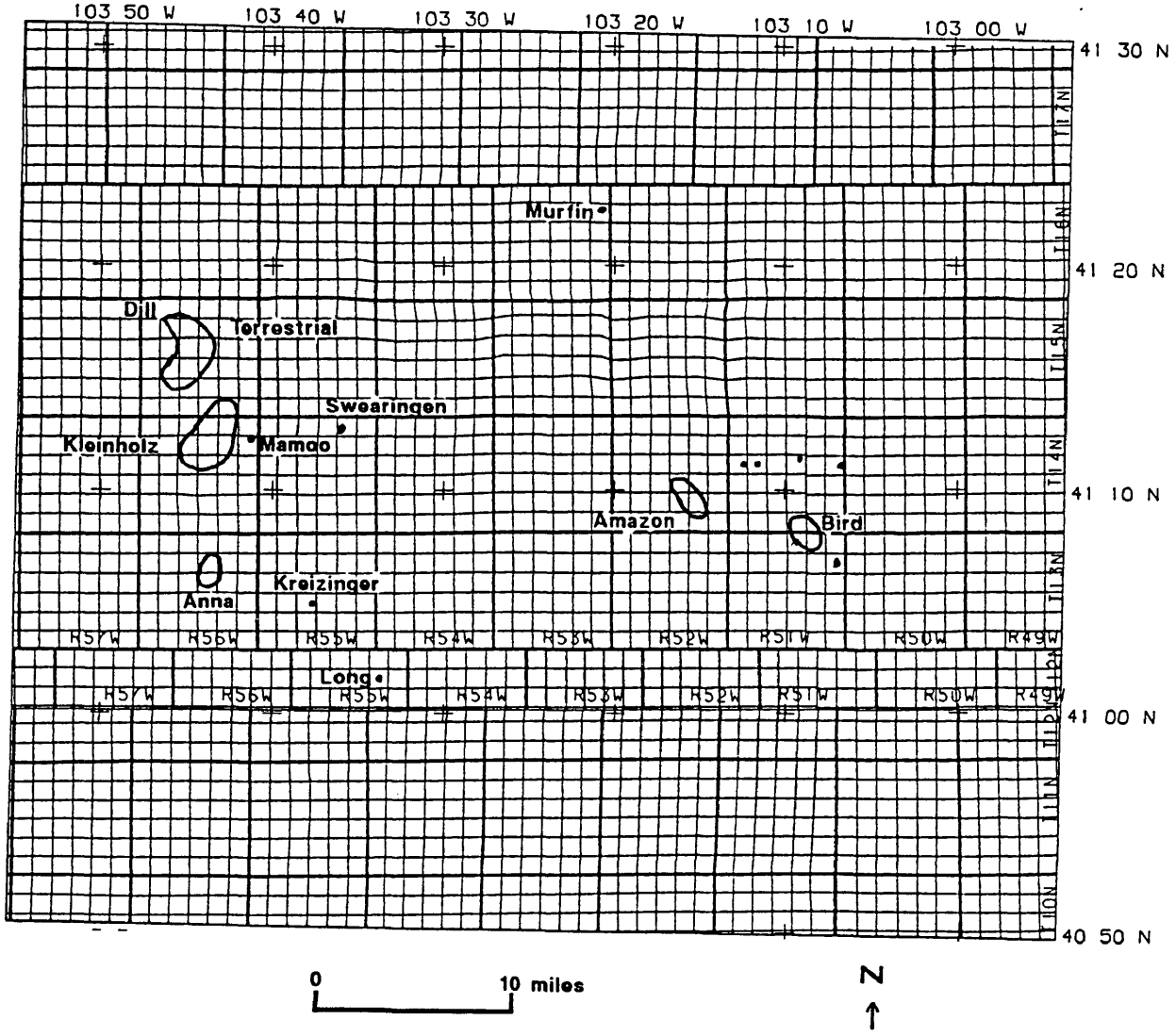

Figure 1. Location of aeromagnetic survey and productive Paleozoic fields

reviews the geology of the Nebraska Panhandle to generate a framework within which these aeromagnetic data can be interpreted. Secondly, this study seeks to identify basement structures and related fracture enhancement that have influenced reservoir potential and deposition of Upper Paleozoic sediments along structurally controlled directions. Thirdly, and most importantly, this research compares the results from a conventional manual interpretation and a neural network automated interpretation of aeromagnetic data to determine the ability of an artificial intelligence system to substitute for a costly, labor-intensive manual interpretation.

Chapter 1

MAGNETIC PROSPECTING AND AEROMAGNETIC SURVEYS

1.1. Magnetic properties

In oil and gas exploration, magnetic methods have been used both to determine the depth to basement in new or unexplored basins and to map positive features that affect the depositional patterns of overlying strata (Dobrin and Savit, 1988). Magnetic data are very useful for determining basement structure because the Precambrian has a quantifiable magnetic response, while the overlying stratigraphic section is almost completely non-magnetic. This is due to the presence, or absence, of magnetic minerals in the composition of the rock. As a result, magnetic surveys effectively see through the stratigraphic column.

Magnetic responses are created because of the magnetic susceptibility of minerals in a body of rock. The susceptibility of a body is a measurement of the degree to which it is magnetized (Nettleton, 1976). Magnetic susceptibility is the critical parameter in magnetic prospecting, just as density is the critical parameter in gravity prospecting. While many minerals possess a measurable magnetic susceptibility, only a few possess significant ones. Of these minerals, the most important is magnetite. To a lesser extent, pyrrhotite and ilmenite are also significant. The magnitude of an anomaly is primarily a result of the composition of the causative geologic body. Since different rock types have varying amounts of these

magnetic minerals, it follows that certain rock types will display observable magnetic responses while others will not. Table 1.1 lists the calculated susceptibilities of many common igneous rocks. As can be seen, although there is a great amount of variation for a given type of rock, there is also a significant amount of overlap between different types. However, Figure 1.1 shows that for different types of rocks, there exists recognizable distinctions. For example, basic and ultrabasic igneous rocks usually possess susceptibilities two or three orders of magnitude greater than sedimentary rocks.

The susceptibility variations within basement, however, are not the only factors in quantifying magnetic anomalies. In a geologic body, increasing the susceptibility only increases the amplitude of an anomaly. Magnetic anomalies are also dependent upon the strike, dip, depth to, and shape of a body. Additionally, the inclination and declination of the earth's field will affect the response (Vacquier et al., 1963). Consequently, by combining these different attributes with available geologic control, it is possible to interpret magnetic fields.

1.2. Remanent magnetization and intrasedimentary sources

In this discussion, remanent magnetization has been heretofore ignored. Magnetic rocks almost always have acquired their fields from the polarization of the earth's field, and their inclination and declination are determined by the present earth's field. Some magnetic rocks, however, display a remanent magnetization that is due to a paleomagnetic field (Dobrin and

Material	Magnetite Content and Susceptibility, cgs units						Ilmenite, average	
	Minimum		Maximum		Average			
	%	$k \times 10^6$	%	$k \times 10^6$	%	$k \times 10^6$	%	$k \times 10^6$
Quartz porphyries	0.0	0	1.4	4,200	0.82	2,500	0.3	410
Rhyolites	0.2	600	1.9	5,700	1.00	3,000	0.45	610
Granites	0.2	600	1.9	5,700	0.90	2,700	0.7	1000
Trachyte-syenites	0.0	0	4.6	14,000	2.04	6,100	0.7	1000
Eruptive nephelites	0.0	0	4.9	15,000	1.51	4,530	1.24	1700
Abyssal nephelites	0.0	0	6.6	20,000	2.71	8,100	0.85	1100
Pyroxenites	0.9	3000	8.4	25,000	3.51	10,500	0.40	5400
Gabbros	0.9	3000	3.9	12,000	2.40	7,200	1.76	2400
Monzonite-latites	1.4	4200	5.6	17,000	3.58	10,700	1.60	2200
Leucite rocks	0.0	0	7.4	22,000	3.27	9,800	1.94	2600
Dacite-quartz-diorite	1.6	4800	8.0	24,000	3.48	10,400	1.94	2600
Andesites	2.6	7800	5.8	17,000	4.50	13,500	1.16	1600
Diorites	1.2	3600	7.4	22,000	3.45	10,400	2.44	4200
Periodotites	1.6	4800	7.2	22,000	4.60	13,800	1.31	1800
Basalts	2.3	6900	8.6	26,000	4.76	14,300	1.91	2600
Diabases	2.3	6900	6.3	19,000	4.35	13,100	2.70	3600

Table 1.1 Calculated susceptibilities (Slichter's method) of rock materials (multiply by 4π to convert to SI units) (from Dobrin and Savit, 1988)

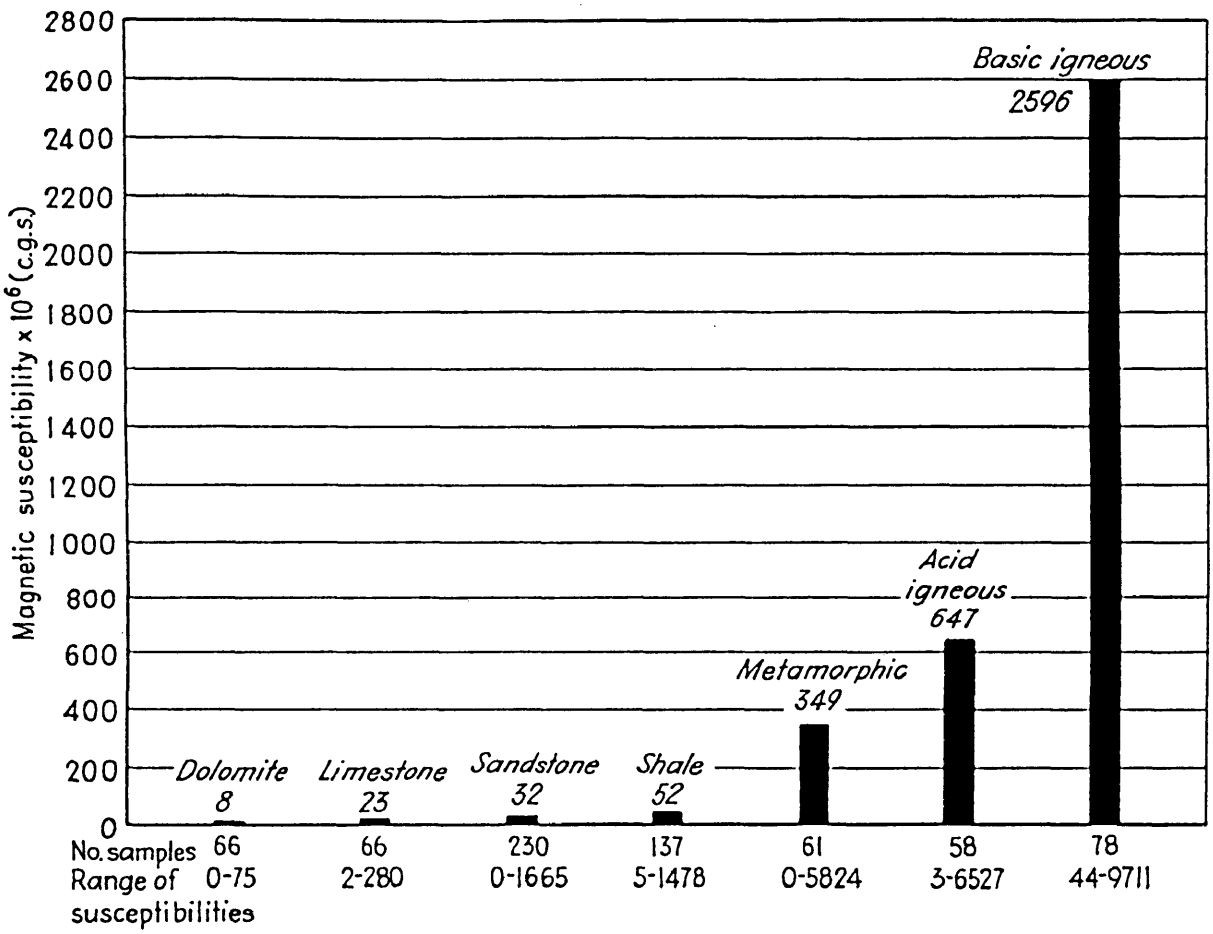

Figure 1.1 Average magnetic susceptibilities for surface samples and cores (from Dobrin and Savit, 1988)

Savit, 1988).

In general, most magnetic anomalies are due primarily to magnetic induction. Remanent magnetization can be extremely important in the interpretation of highly magnetized bodies such as diabase dikes, volcanics, and younger mafic intrusives (Hinze and Zietz, 1985). In areas where these highly magnetized materials are absent, remanent magnetization can generally be ignored (Nettleton, 1976). Several case studies from areas that are dominated by acidic igneous rocks corroborate this.

A study of outcrops of the Spavinaw granite in Oklahoma demonstrated that remanent magnetization occurred in random directions and that its effects were completely cancelled at an observation elevation of 250 meters (Hawes, 1952). Currie et al. (1963) found in a study of Cretaceous granites in the Sierra Nevada that magnetic susceptibility determines the nature of the magnetic anomalies encountered. Allingham and Zietz (1962) undertook a study of the Climax stock in Nevada and found that remanent magnetization of this intermediate intrusive body had intensities less than one-eighth that of the induced magnetization and random scattering of direction. Since the basement of the Nebraska Panhandle is dominated by similar felsic rocks, remanent magnetization in the basement has been ignored for this study.

Although the Precambrian basement is by far the most significant source of magnetic anomalies, the effects of intrasedimentary induced and remanent magnetization must also be considered. The presence of highly magnetized material, such as volcanic layers and detritus

derived from mafic protoliths, within the stratigraphic column can create magnetic anomalies of significant amplitude.

Within the study area, red beds of Permian age do exist. These red beds form a continuous blanket across the study area (pers. comm., R. Weimer, 1996). Forward modelling of a thin, laterally continuous magnetic sheet shows that the only anomaly due to induction occurs along the edges of the sheet (Telford et al., 1990). Since the limits of the red beds are not within the survey area, there should be no significantly associated induction anomaly (Figure 1.2). Diagenetic reactions have converted what magnetite that was present into hematite. Within Permian sandstones, the paleomagnetic field is nearly horizontal and any remanent magnetization is of such small magnitude that it is undetectable (Larson et al., 1982).

To distinguish further the effects of intrasedimentary magnetic sources, a Wiener filtering operation was performed on the total magnetic intensity data. Using an in-house Wiener filter program, a three-layer magnetic model was created for the study area. The program is based on the idea that the statistical properties of the magnetic spectrum can be modeled by distributions located at a few depth horizons. The magnetic spectrum then has slope breaks between segments corresponding to different depths. The segments are fitted by standard least-squares methods. The results of this operation show that the sources for the top layer are above the ground, the middle layer are in the sedimentary section (~1,000 meters), and the bottom layer are deep within the Precambrian (~4,400 meters). A comparison of the deep

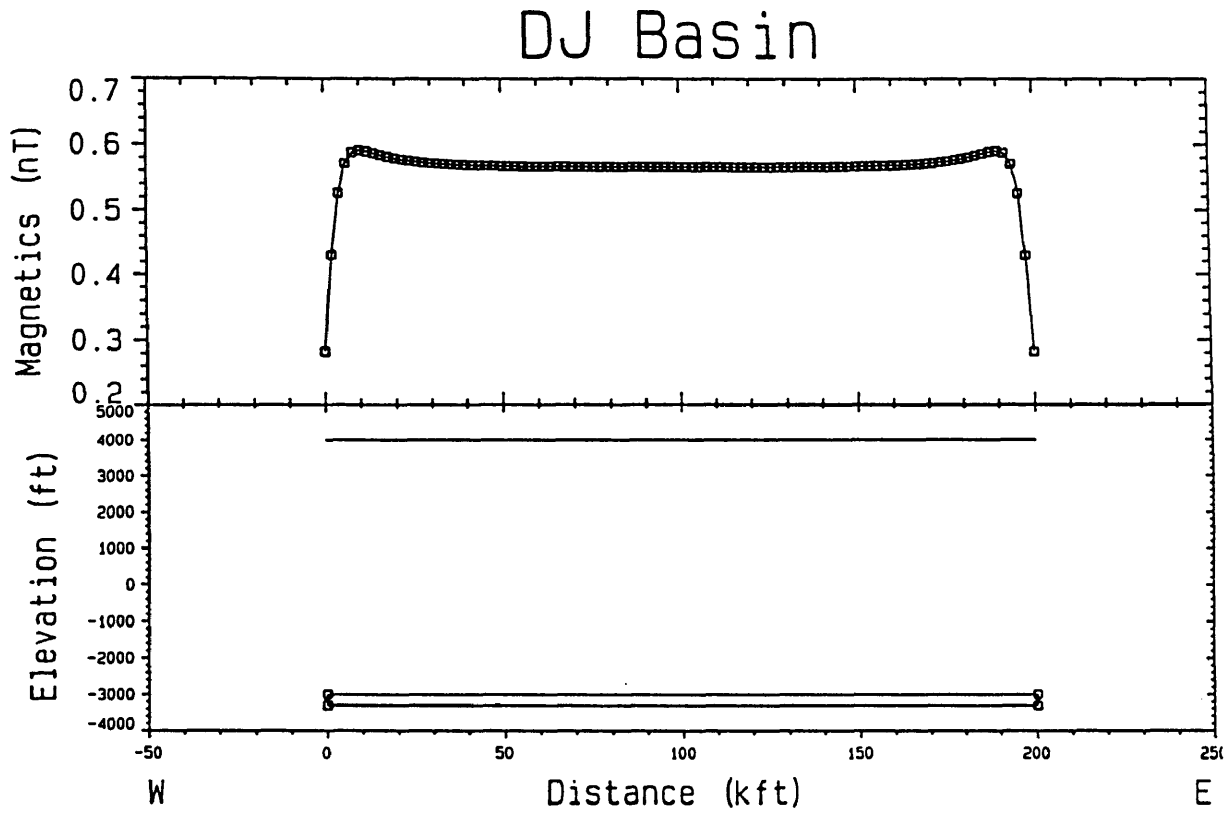

Figure 1.2. Forward magnetic model of a thin, laterally continuous sandstone sheet with susceptibility of 300 μcgs (3.8×10^{-3} SI) units

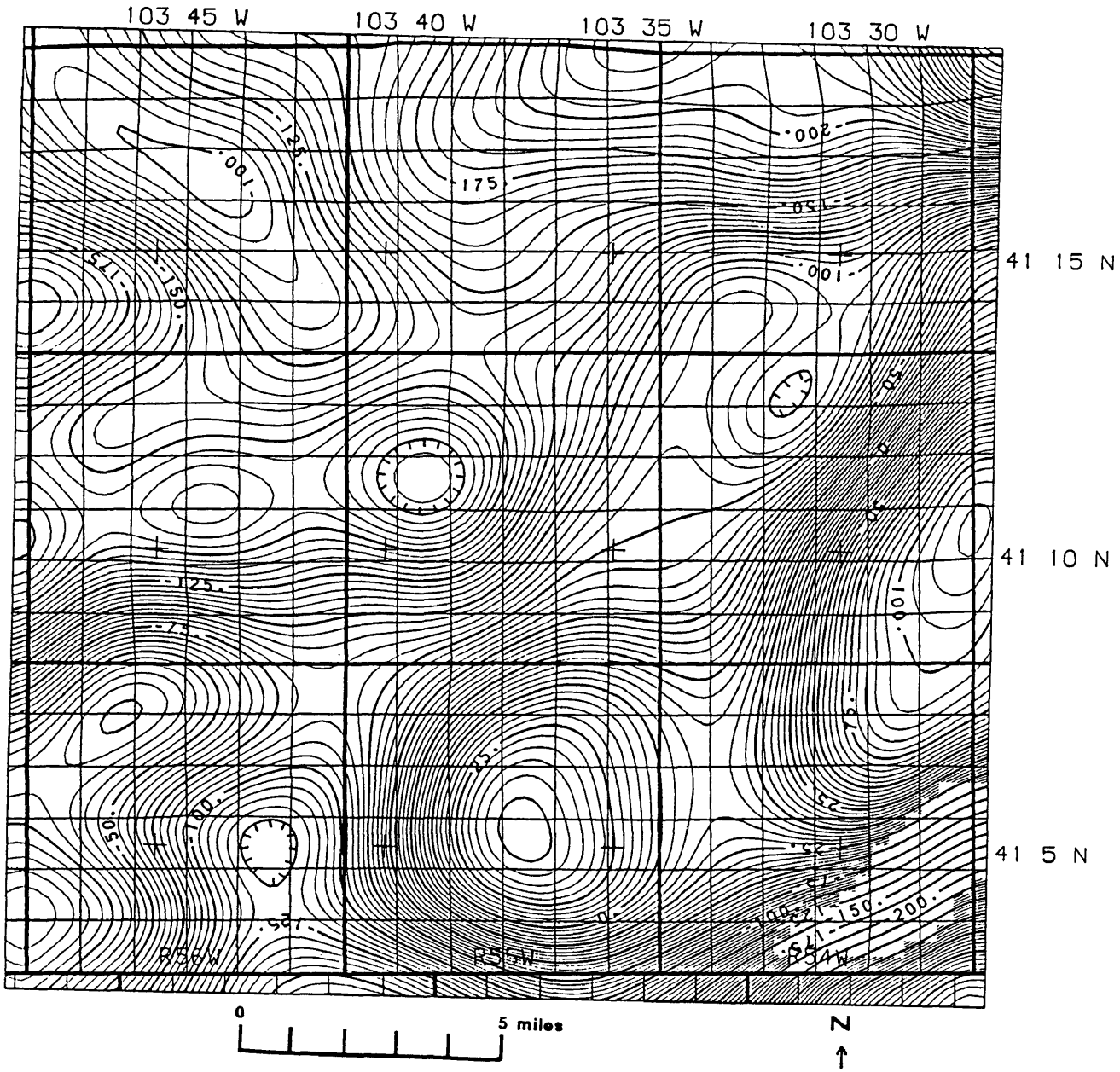

Figure 1.3 Deep component of observed magnetic field
(Contour interval = 5 nT)

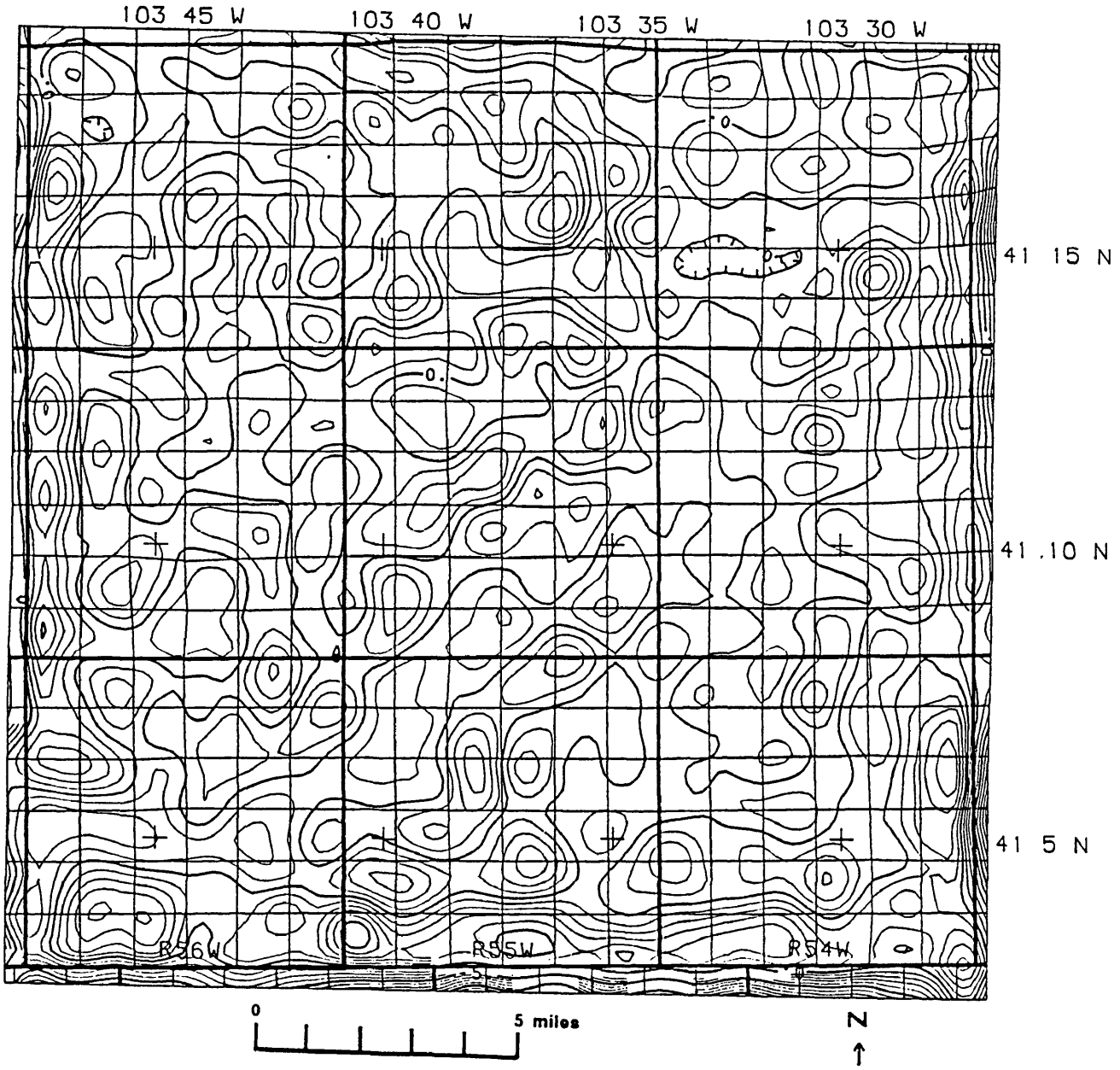

Figure 1.4 Intrasedimentary component of observed magnetic field (Contour interval = 1 nT)

component of the magnetic signal (Figure 1.3) with the observed magnetic response (Figure 3.2) confirms that Precambrian basement is the primary source of all observable magnetic anomalies. A map of the intersedimentary layer's contribution, however, shows only random noise (Figure 1.4). Hence, intrasedimentary sources do not figure into the interpretation of these magnetic data.

1.3 Magnetic anomaly characterization

Since magnetic anomalies are dependent upon many variables, it is possible to distinguish different types of sources by considering the character of the magnetic field. For example, intrusives generate low-frequency anomalies because of their great depth extent. The amplitude of the feature will increase as the intrusive becomes more basic. Conversely, cultural sources can also produce a high amplitude anomaly, but their frequency will be very high. Thus, it will be difficult, if not impossible, to correlate cultural anomalies from one line to another. Aside from cultural anomalies which are removed from a survey prior to processing and interpretation, there are three primary sources of magnetic anomalies: (1) intrabasement lithology changes, (2) suprabasement structural features, and (3) a combination of these two sources. Because susceptibility variations due to intrusions have great depth extent, the resultant anomaly will have a low frequency. When compared with intrabasement lithologic anomalies, structural anomalies do not possess any depth extent and, therefore, possess a higher frequency content. The detection of either faulted basement structures or

positive basement features along aeromagnetic profiles, therefore, requires the separation of low-amplitude, high-frequency structural anomalies from high-amplitude, low-frequency intrabasement lithologic anomalies.

1.4 Aeromagnetic survey

The acquisition of a high-quality survey is of paramount importance if small, high-frequency anomalies are to be isolated. This high-resolution survey over the Denver-Julesburg Basin was acquired in 1987 by Airmag Surveys, Inc. of Philadelphia, Pennsylvania. A fixed-wing aircraft maintained a constant mean terrain clearance of 300 feet and sampled the magnetic field approximately every 60 feet. Since the survey was flown before the widespread use of GPS navigation, video flight path recovery was used. Table 1.2 shows the data acquisition parameters.

After the data were acquired, they were processed to ensure that the high-frequency signal component was not lost during despiking and deculturing of the data. Flight line and tie line intersections were minimized by applying both a DC level shift and a first-order polynomial to individual lines. After intersection misties were brought within an acceptable range, the International Geomagnetic Reference Field (IGRF) correction was performed, and the data were mapped. Data enhancement techniques including reduction to the pole, susceptibility inversion, and horizontal and vertical gradients were all subsequently performed but will not be considered until after examining the geologic framework into which the magnetic data fit.

Contractor	Airmag Surveys Inc. Philadelphia, Pennsylvania
Date of Survey	The main body of the survey was flown in 1987. Three extensions were flown in March, 1993.
Flight Pattern	Flight lines: 0.5 mile spacing (east-west) Tie lines: 1.0 mile spacing (north-south)
Mileage	4,360 line-miles total (1987 and 1993 surveys)
Flight Altitude	300 ft ground clearance
Aircraft	Twin engine Cessna 320 with stinger
Airborne Magnetometer	Optically-pumped Cesium vapor magnetometer (0.01 gamma sensitivity)
Ground Magnetometer	Same
Altimeter	Honeywell 7505 radar altimeter plus Rosemont barometric altimeter
Fiducials	0.25 second readings
Navigation	35 mm continuous strip correlated to 7.5 minute topographic maps for 1987 survey. G.P.S. multichannel Trimbel receiver for 1993 survey.

Table 1.2 Aeromagnetic data acquisition parameters

Chapter 2

GEOLOGY OF THE NEBRASKA PANHANDLE

2.1 Introduction

In any geophysical interpretation, an understanding of the geology of the area is critical. In magnetic prospecting for oil, a thorough understanding of the basement rocks is of highest importance. This is because the primary source of magnetic anomalies is from within Precambrian basement (Nettleton, 1976). Although there may be magnetic sources in the stratigraphic column and at the surface due to cultural features, the primary magnetic source is from the Precambrian. Within the basement, magnetic anomalies may originate from several sources: (1) lithologic, or susceptibility, variations, (2) structural relief upon the Precambrian surface due to paleotopography, (3) structural relief due to rejuvenation of fault blocks along pre-existing planes of weakness, or (4) a combination of some or all of these. Because of the non-uniqueness of determining the source of magnetic anomalies, it is critical to understand the geology of the area, especially with regard to basement, prior to interpreting an aeromagnetic survey.

2.2 Study area and regional geology

The study area is in the panhandle of Nebraska and lies in a part of Kimball County (Figure

2.1). This area is part of the Denver-Julesburg Basin, a large north-south elongated foreland basin that owes its current shape to the Laramide orogeny. The basin is highly asymmetrical with its axis close to the mountain front. The western margin is steep and exhibits structural features that are related to the orogeny. Conversely, the eastern margin dips gently to the west (about 30 to 60 feet per mile at the top of the Pennsylvanian) and exhibits features of an interior cratonic basin (Rogers and Logan,1988). The basin is bounded by the Laramie and Front Ranges to the west, the Chadron Arch to the northeast, the Cambridge and Las Animas Arches to the southeast, and the Apishapa Uplift to the south (Figure 2.2).

The Denver-Julesburg basin is a structural feature of first order. Second and third order features were superimposed on the first order feature (Figure 2.3). These features were preferentially emplaced along zones of weakness that were present from earlier tectonic movement in both Paleozoic and Precambrian time. These second and third order features create local structural influences on deposition. When these areas are subjected to recurrent movement along basement faults throughout geologic time, structural and stratigraphic traps can be created. Earlier work on this subject was performed in the Paradox Basin (Baars, 1967) and in three other Colorado basins (Weimer, 1980a). Consequently, it is important to examine the history of these zones of weakness.

2.3 Precambrian geology

Within the study area, the Precambrian basement is completely covered with Phanerozoic

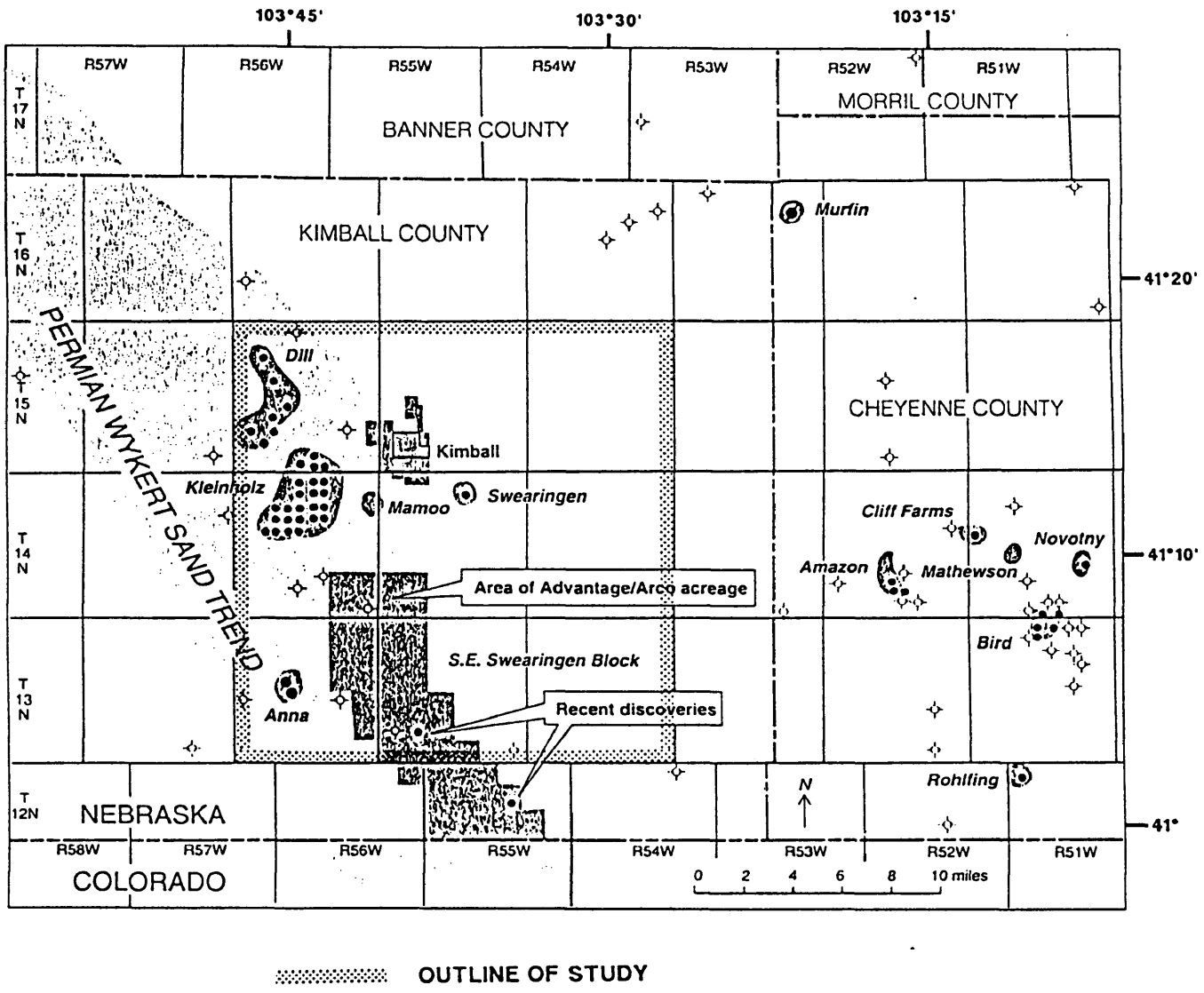

Figure 2.1 Study area
(adapted from Hart, 1992)

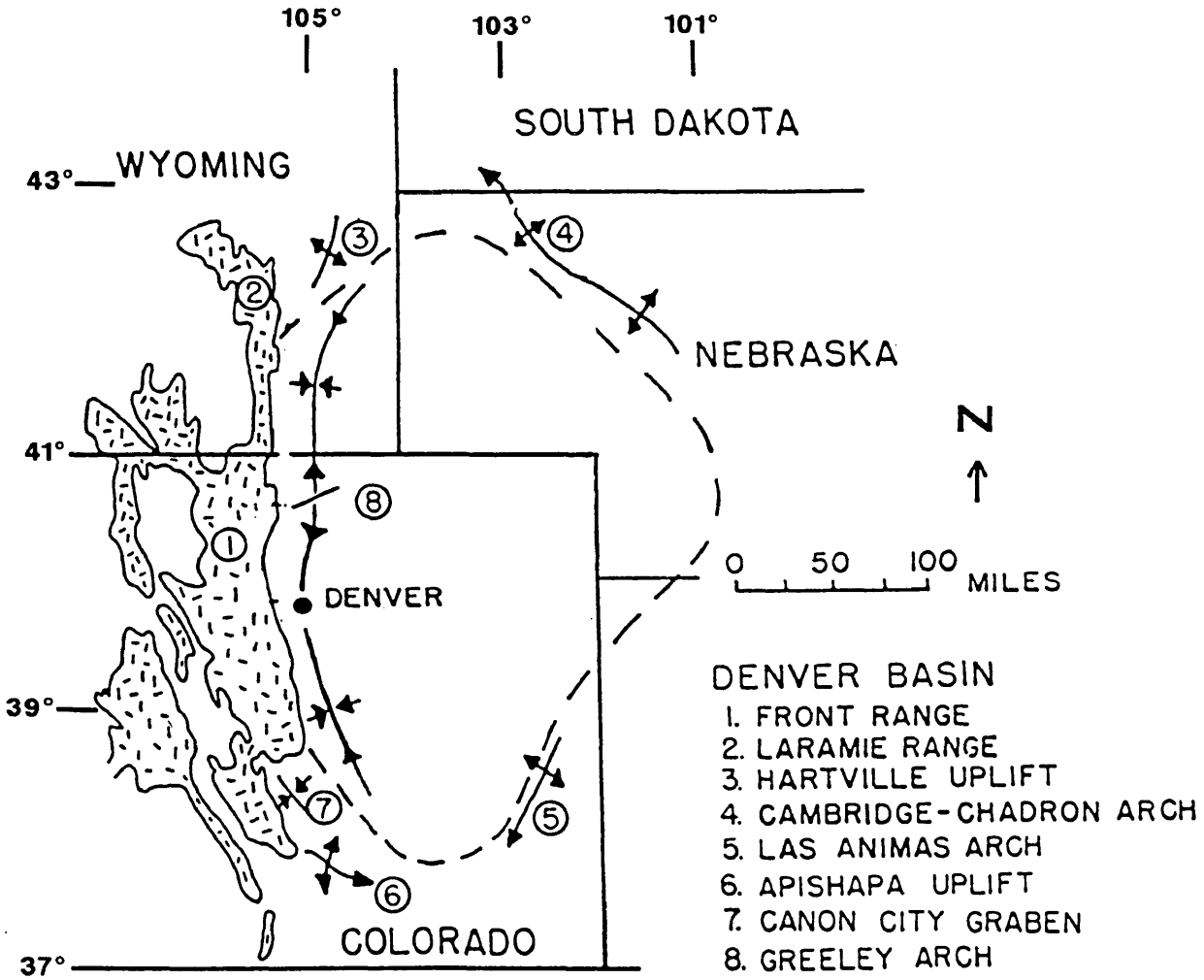

Figure 2.2 Denver-Julesburg Basin and bounding structural features (from Sonnenburg and Weimer, 1981)

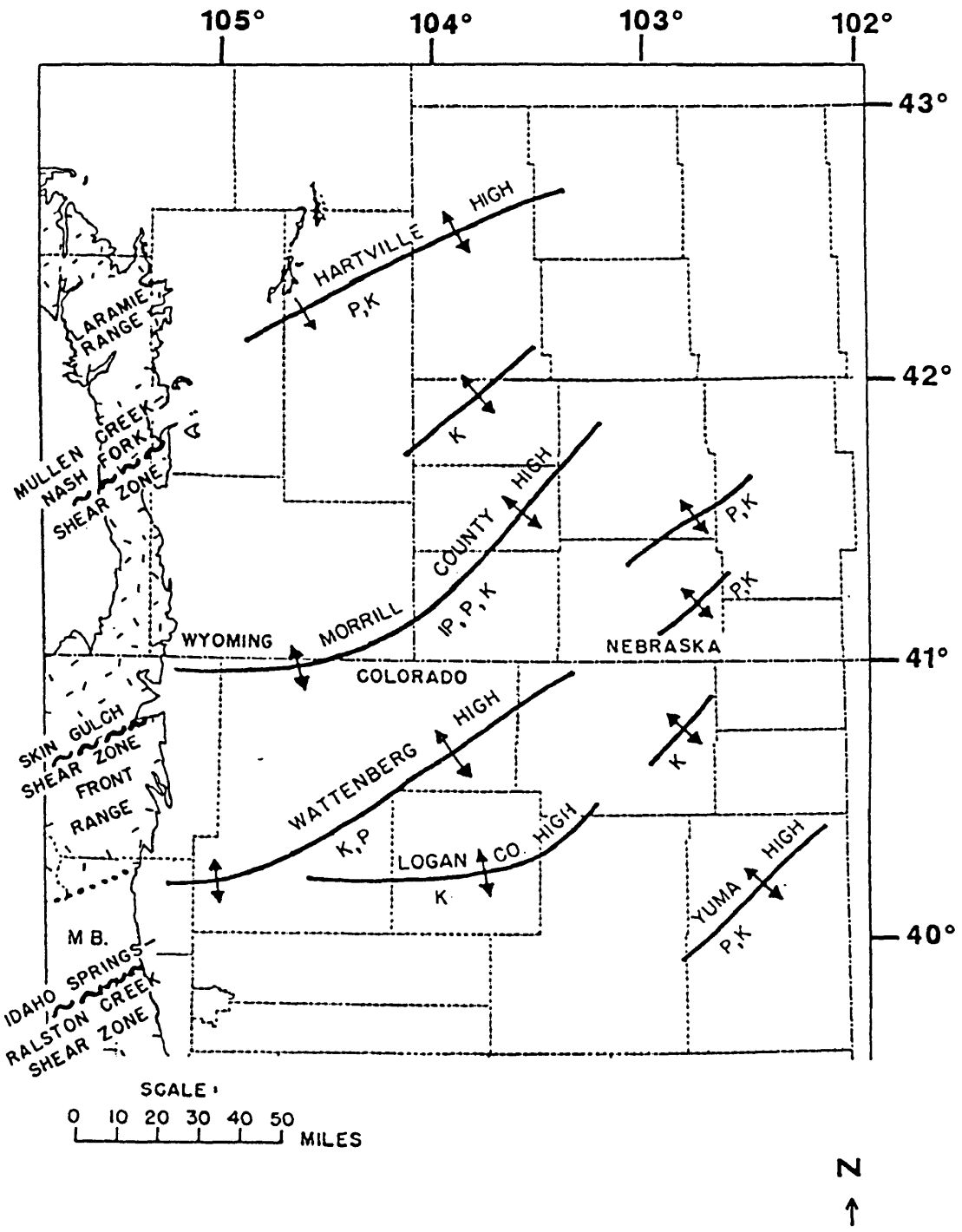

Figure 2.3 Subordinate structural features within the Denver-Julesburg Basin (from Sonnenberg and Weimer, 1981)

strata. Most knowledge of the basement depends primarily upon oil test boreholes. While many papers have been written upon the subject (Edwards, 1963, Lidiak, 1973, Tweto, 1980b, and Sonnenberg and Weimer, 1981), a brief review of Precambrian geology is appropriate.

The oldest Precambrian rocks are approximately 1,800 million years in age and are gneisses that have been metamorphosed to amphibolite stage (Tweto, 1980b). These rocks are primarily medasediments and metavolcanics. The protoliths for the metasedimentary gneisses were greywackes and shales. The metavolcanic gneisses are of two rock types, (1) amphibolite gneisses derived from tuffs, lavas, and breccias from intermediate to basic composition, and (2) felsic gneisses derived from tuffs and dikes of silicic composition. The metamorphic rocks have a minimum age of 1,700 million years, since geologic analysis shows that metamorphism occurred prior to, and during, emplacement of the first major igneous intrusion of that age. These metamorphic rocks may date back as far as 2,600 million years based upon outcrops in the Sierra Madre Range of southern Wyoming (Love and Christiansen, 1985). The metasediments and metavolcanics, therefore, serve as a matrix into which later Precambrian events were fit.

The igneous rocks that were first intruded into this metamorphic matrix are known to have a wide range of compositions but are primarily granodiorites and quartz monzonites. Lidiak (1972) states that cores from wells in Sioux and Grant Counties have age dates that suggest the intrusives in the basement were emplaced at the same time as those in both the Front

Range and Black Hills. In the Nebraska Panhandle, the primary igneous rock is of granitic composition and is assumed to have the same genesis. A second occurrence of igneous rocks that is south of the study area is a localized intrusion of granite that has an approximate age of 1,400 million years.

Borders between lithologic provinces are sharp and may be fault controlled. Tweto (1980a) states that portions of the northwest trending fault system were present before intrusion of the 1,700 million year granite and that, although the northeast system was primarily active after the 1,400 million year intrusion, this too may have originated earlier. Baars and Stevenson (1981) date the northwest trending features at 1,700 million years, and Warner (1978) dates the northeasterly trend at 1,700 million years also. Considering that the orientations of granitic provinces within the study area are directed along this pair of axes, it can be inferred that these structural directions were already present before intrusion of the oldest granite (Figure 2.4). Hence, structural controls that influenced Phanerozoic depositional patterns were already embedded in the Proterozoic.

2.4 Lower Paleozoic geology

Within the study area, Precambrian rocks are unconformably overlain by Pennsylvanian sediments. Elsewhere in the basin, however, several hundred feet of Cambrian to Mississippian sediments are present. Sonnenberg and Weimer (1981) discuss these rocks, and for this study it is worth noting their depositional patterns. Cambro-Ordovician rocks, where

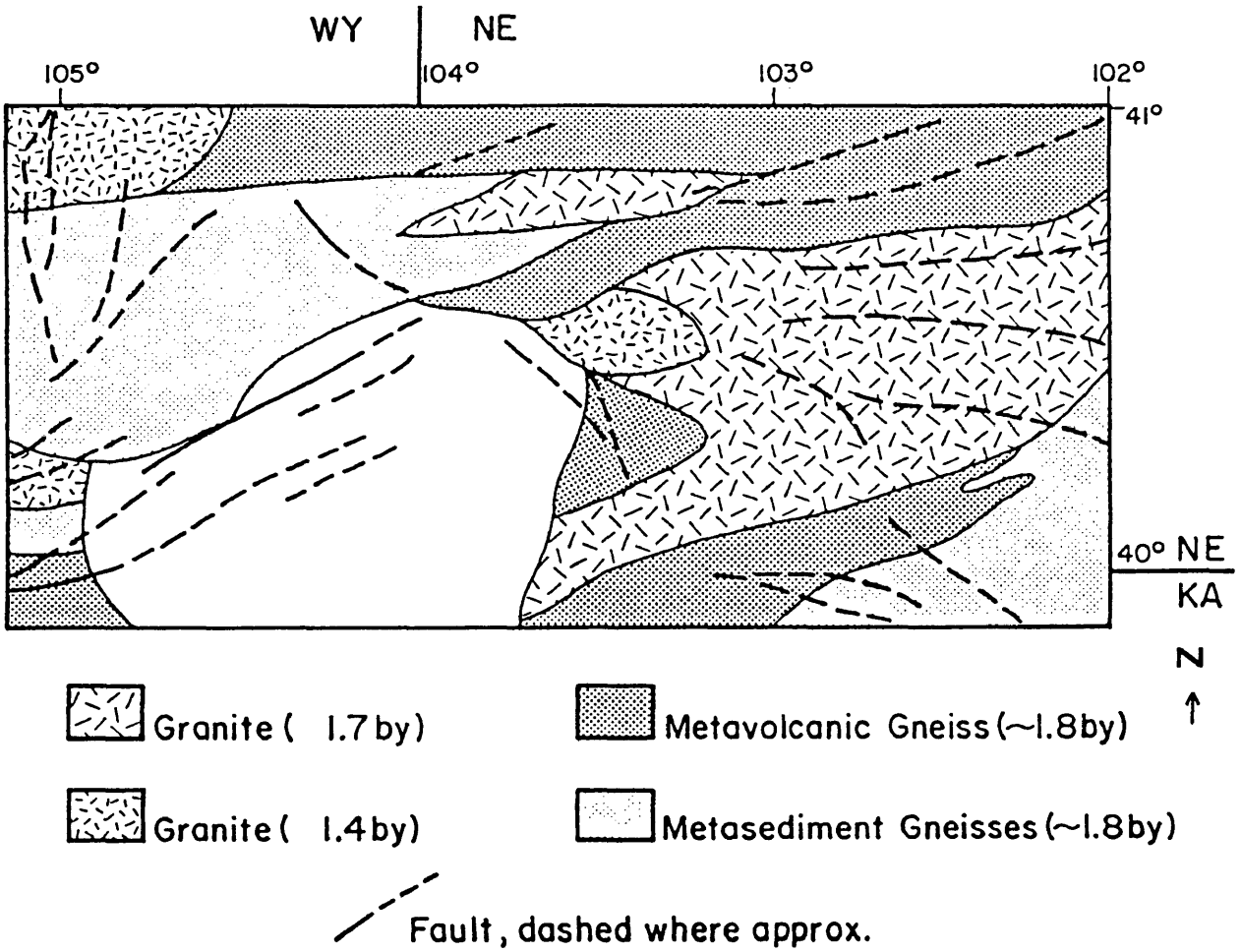

Figure 2.4 Precambrian lithologic boundaries in northeastern Colorado (modified from Tweto, 1980b)

present, are oriented in a northeasterly trend (Figure 2.5). Although evidence points to the fact that rocks of this age were possibly widespread in the Nebraska Panhandle and both eastern Wyoming and Colorado, reactivated uplift along the northeast trending Transcontinental Arch in Silurian time eroded away these sediments.

Similarly, patterns of Mississippian deposition indicate preferential northwest and northeast alignments (Figure 2.6). Uplift along northeast trending fault zones removed most of these sediments prior to Pennsylvanian time, but within a northwest trending graben-like feature (the Morgan County Low), over 100 feet of Kinderhookian and Osagian strata are preserved.

Within the basin, lower Paleozoic strata are not known to be oil productive. Correlative units of Mississippian age in the Paradox Basin are highly productive but are much more widespread. As a result, there exists the potential for production in the Denver-Julesburg Basin, pending further exploration of these intervals.

2.5 Pennsylvanian and Permian periods

Lower Paleozoic tectonic features are not prevalent in the study area, with exception of the Transcontinental Arch (Ross and Tweto, 1980). During Pennsylvanian time, however, a period of intense tectonic deformation occurred. With uplift of the Ancestral Front Range and downwarp of the craton to the east, the current Denver-Julesburg Basin first took shape. The Chadron Arch, the northeastern bounding structure of the basin, was upwarped and

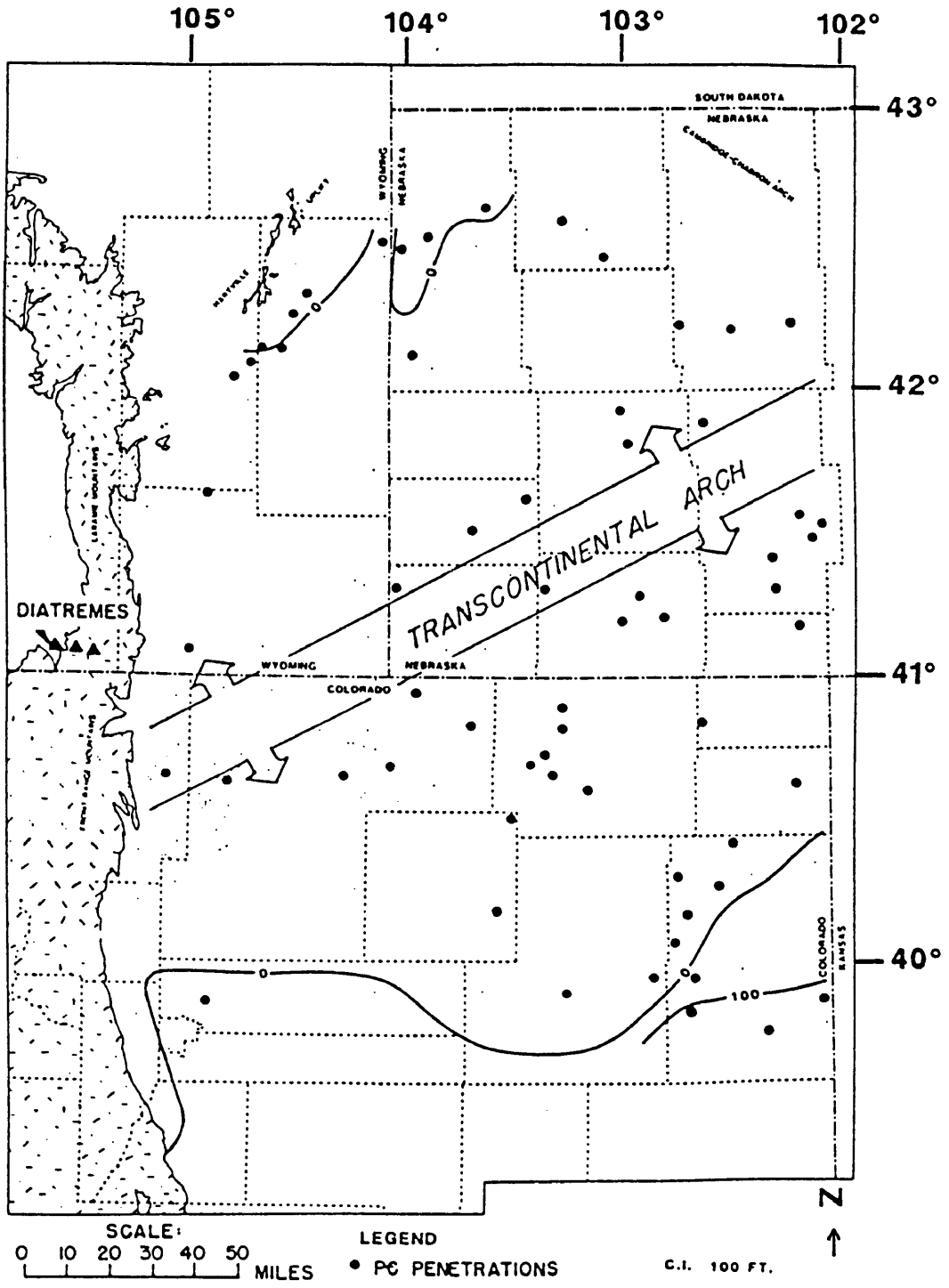

Figure 2.5 Depositional patterns of Cambro-Ordovician sediments (from Sonnenberg and Weimer, 1981)

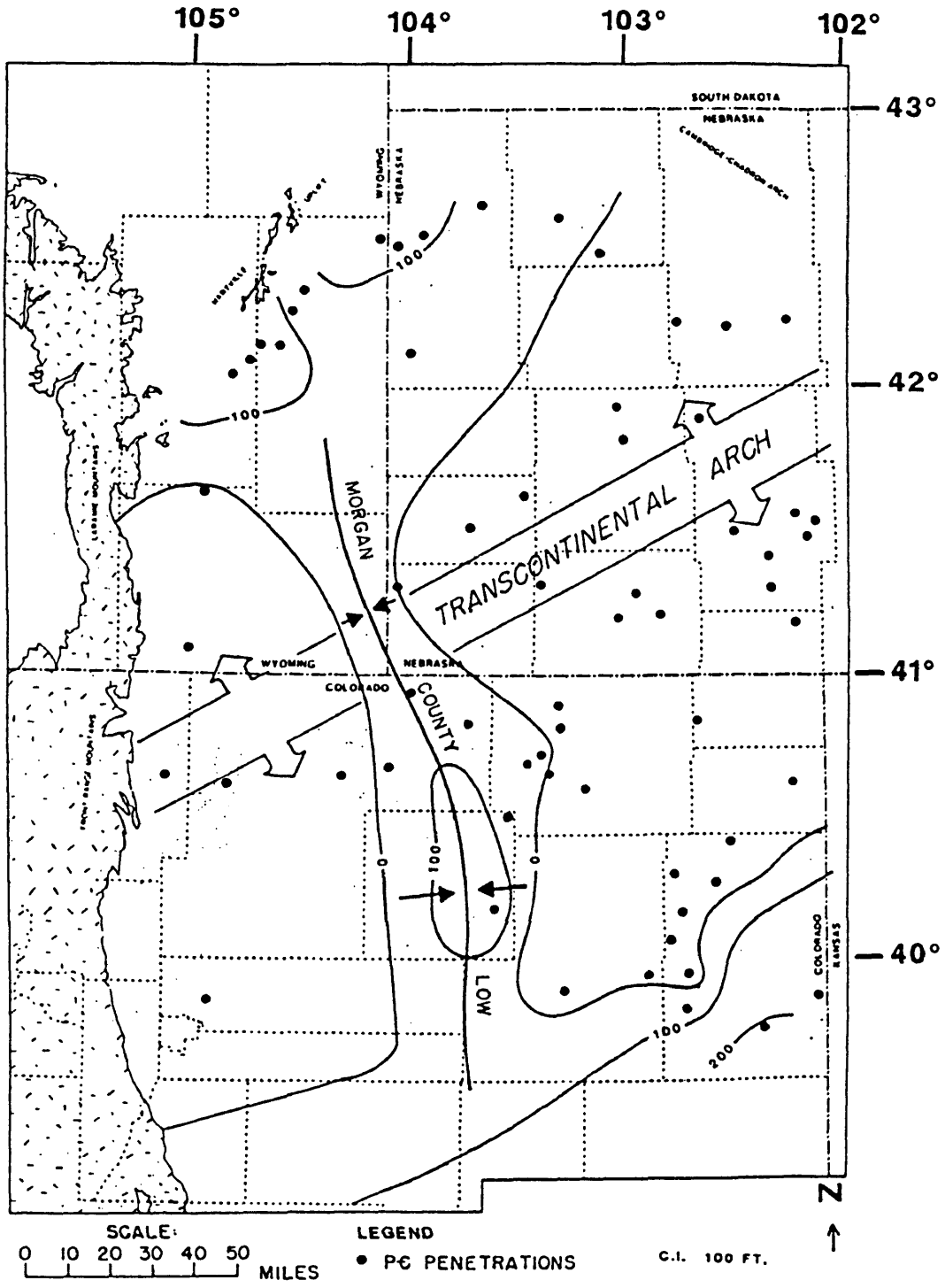

Figure 2.6 Isopach of Mississippian sediments (from Sonnenberg and Weimer, 1981)

eroded to Precambrian basement in early Pennsylvanian time (Baars et. al., 1988). Additionally, structural blocks along the western flank of the basin were downdropped, producing rapidly changing depositional centers (DeVoto, 1980). Within western Nebraska, the shelf margin dipped very gently to the southwest. Thus, the superposition of tectonic features greatly affected local stratigraphy.

Late Paleozoic rocks include Pennsylvanian and Permian sediments ranging from probable Morrowan to Atokan and Guadalupian age (Momper, 1963). Morrowan to Atokan rocks unconformably overlie Precambrian rocks in the study area. To the east, the Precambrian is on-lapped by progressively younger (Cherokee Age) Pennsylvanian rocks, which are in turn beveled by a minor unconformity (Hoyt, 1963 and Momper, 1963).

The Transcontinental Arch was a significant feature that formed a sill, effectively dividing the Denver-Julesburg into two sub-basins, and restricting circulation between the Alliance and Sterling Basins periodically during Pennsylvanian and Permian time. As a result, sediments in the Alliance Basin tend to be more evaporitic and dolomitic than contemporaneous sediments in the Sterling Basin to the south (Hoyt, 1963, and Momper, 1963).

The basal Morrowan-Atokan sequence is composed of interbedded, marine and fluvial sandstones, red to green shales, and minor subtidal, cherty carbonates. The overlying Desmoinesian to Wolfcampian strata are composed of shallowing and locally "brining" upward cycles, consisting of interbedded gray to light brown, locally cherty limestone,

dolomite, sandy dolomite, dolomitic sandstone, anhydrite, salt, gray to black shale, and red to greenish siltstone. The cycles are similar to the typical Kansas cyclothems described for the Lansing-Kansas City Group of the Midcontinent (Watney, 1980), with the exception that the basal (transgressive) portion of the cycle is commonly lacking or severely abbreviated. This is probably due to the often shallow and intermittent flooding of the Transcontinental Arch. Permain sequences to the north and west are dominated by clastics, whereas sedimentation in the the Midcontinent, being more distant from active major source areas, consists of numerous distinct clastic/carbonate, clastic/evaporite, and carbonate/evaporite cycles.

Deposition of the cycles within the Desmoinesian through Wolfcamp interval typically began with a rapid transgression, followed by deposition of subtidal and intertidal carbonates and siliclastics during a relatively slow regression. The rapid transgression and predominance of inner shelf depositional environments resulted in abbreviation of the deeper marine portion of the depositional cycle. Locally, black marine shales deposited under euxinic conditions during maximum transgression are preserved. These potential source rocks can be recognized on logs by an abnormally high gamma ray response. Several of these characteristic shales are present at the top of the Cherokee. Additional black shales underlie the Mamoo zone in the Upper Virgil. Not only are these shales excellent hydrocarbon source rocks, they also form excellent seals.

The lower portions of the depositional cycles are typically sharply overlain by low to

moderate energy subtidal carbonates. These may grade upward or be sharply overlain by moderate to locally high energy carbonates. Abraded fossil fragments, ooids, and peloidal grainstones may be common to abundant. These may be overlain in turn by low energy intertidal carbonates (with algal laminations, fenestral fabric, and brecciation texture), siltstones, red to greenish gray shales, nodular to massive anhydrite (Upper Virgil to Permian), or salt (Leonard to Guadalupian age sediments).

The often undifferentiated Wykert Sand represents a change in depositional setting from that of the underlying Pennsylvanian and Permian carbonates. Recently published information suggests that the Wykert was deposited along a marine shoreline, during the transgressive reworking of eolian sand derived from the north and east (Hart, 1992). In this regard, the Wykert Sandstone is similar in character to the Leo sands of the Minnelusa, which produce in the southwestern portion of South Dakota.

From Desmoinesian through latest Permian, the sediments became less normal marine in character with an increase in more restricted marine (dolomite) to evaporitic and continental lithofacies. Evaporites appear lower in the stratigraphic section in the Alliance Basin to the north, reflecting the influence of the Transcontinental Arch. The uppermost Permian rocks (Leonardian and Guadalupian) consist of silty and shaly red beds, anhydrite, sandstone (Lyons), and minor carbonates with highly variable amounts of halite. The Lyons Sandstone (Leonardian) occurs as eastward thinning pods of eolian dune sand aligned along the trend of the Transcontinental Arch (Sonnenberg and Weimer, 1981).

Rejuvenation of old fault blocks continued to localize deposition.in areas such as the Morgan County Low and created both positive and negative structures along preferential trends (Figures 2.7 and 2.8). Because of the extremely gentle dip of the eastern margin of the basin, these structural features that correlate with Precambrian ones were critical in localizing both topographic and bathymetric highs and lows, which in turn, localized the development of different depositional environments, including tidal flats, subtidal deposits, and Permian dunes (Montgomery, 1987). The chance of discovering further production in Paleozoic rocks of the basin, therefore, can be improved by a thorough understanding of the relationship between the depositional and tectonic histories that determine reservoir potential.

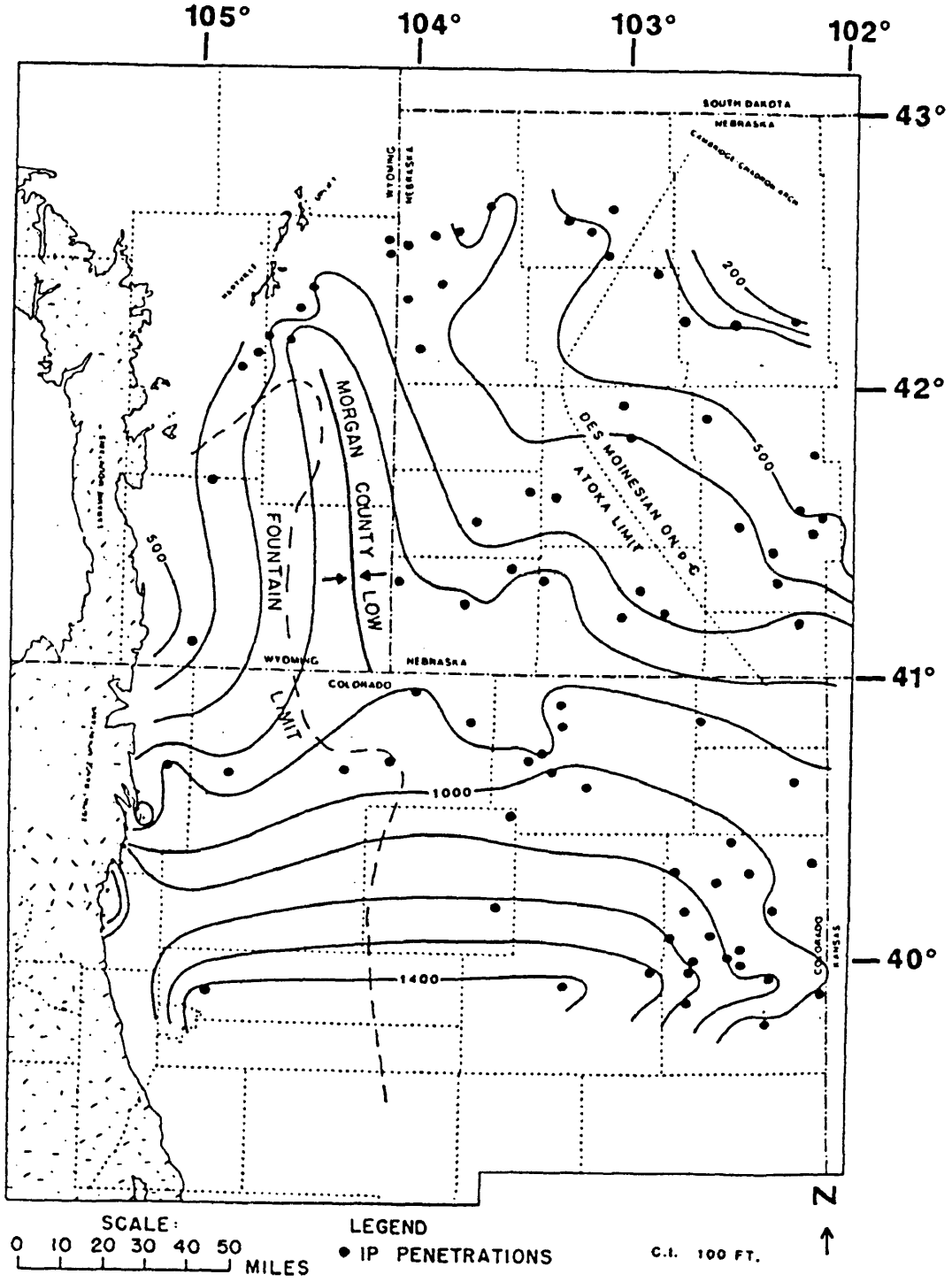

Figure 2.7 Isopach of Pennsylvanian sediments (from Sonnenberg and Weimer, 1981)

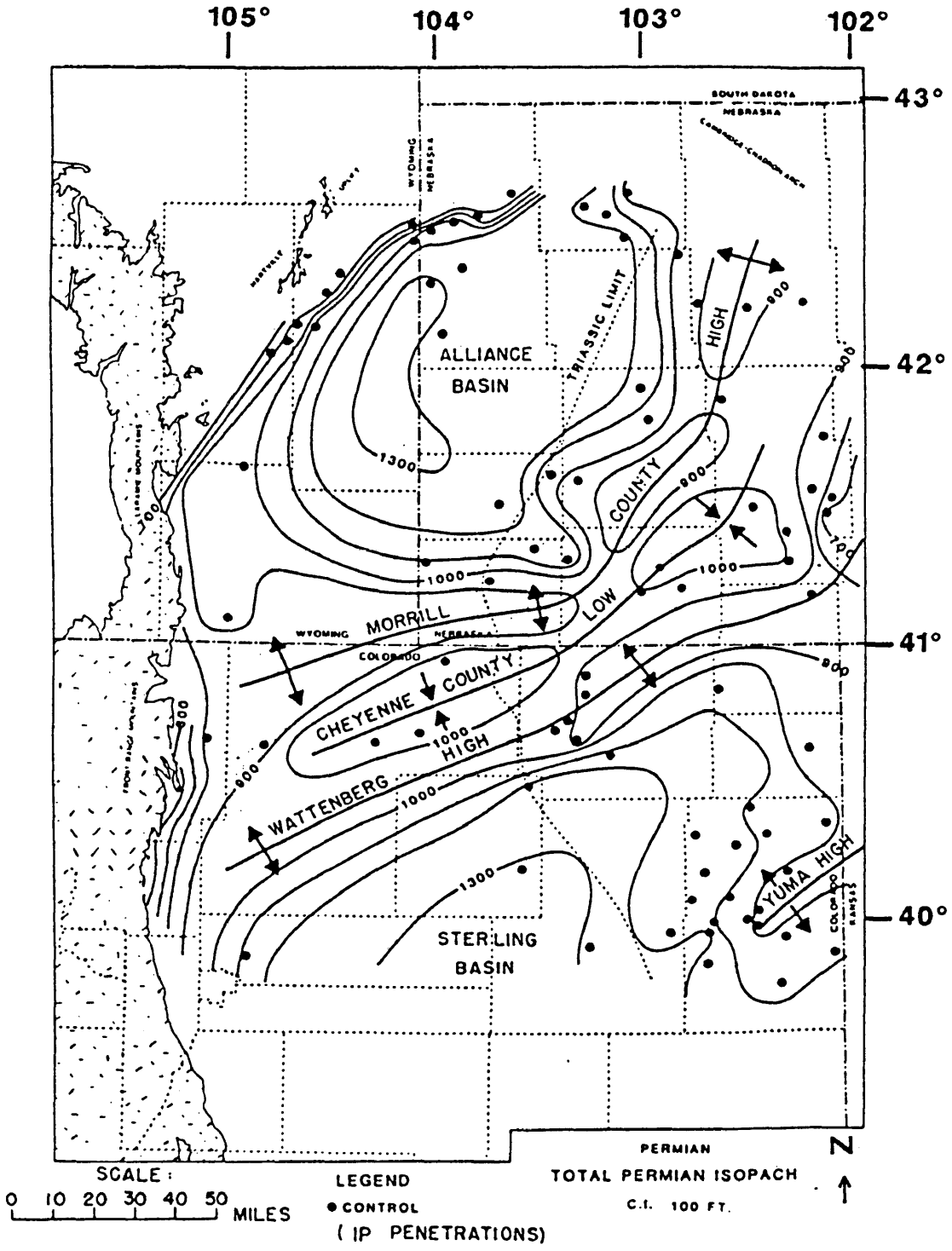

Figure 2.8 Isopach of Permian sediments
(from Sonnenberg and Weimer, 1981)

Chapter 3

THREE-DIMENSIONAL DATA ANALYSIS

3.1 Introduction

The heterogeneity of the Precambrian geology of the Nebraska Panhandle can be mapped accurately with an aeromagnetic survey if the survey is closely spaced and prudently processed. Basement structures and faults that influenced the paleotopography during the deposition of source and reservoir rocks can be identified. The presence of these paleotopographic highs and lows created structural closures and stratigraphic pinchouts that could serve as hydrocarbon traps. Because of the ambiguity of potential field data, however, geologic control should be incorporated into the interpretation wherever possible. Therefore, oil and gas production data, formation tops, and structural information from wells in the Nebraska Panhandle were incorporated into the study. For wells that penetrated it, the depth to the top of Precambrian was recorded. From these points, a first order Precambrian surface was generated.

3.2 Three-dimensional data analysis

Figure 3.1 is a flight line map of the aeromagnetic survey. As briefly mentioned in Chapter 1, several forms of editing were performed on the profile data before mapping. These techniques included flight path recovery, the location of average velocity deviations that

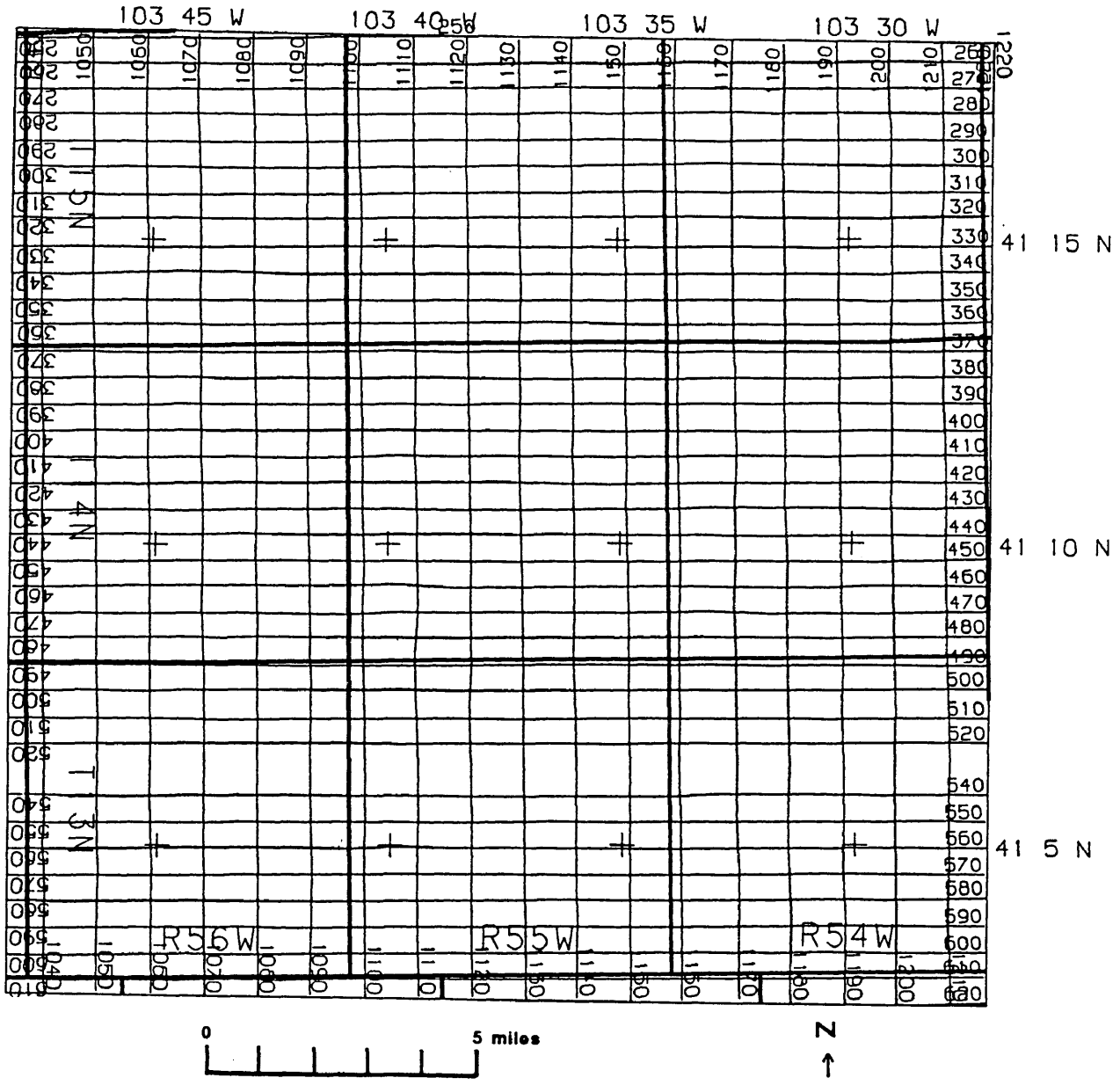

Figure 3.1 Flight line location map

indicate navigation errors, deculturing and despiking of the profile data, diurnal removal, and zero and first order line levelling. These processing steps were performed in order to ensure that when mapped, the data would have the highest signal to noise ratio possible.

3.2.1 Total magnetic intensity map

Figure 3.2 is a map of the total magnetic intensity across the study area. The total magnetic intensity map has had the International Geomagnetic Reference Field (1990 version) removed and shows a magnetic relief of approximately 400 gammas across the map. Areas of strong positive anomalies are likely areas containing locally higher susceptibility Precambrian rocks. Similarly, the large, broad magnetic lows are likely areas of lower susceptibility Precambrian rocks. While these broad magnetic highs and lows are probably resultant mostly from lithologic variations in basement, a degree of structural variation may also be present in these anomalies. It is certain, however, that the biggest anomalies are not caused exclusively by suprabasement features, as the lateral and vertical constraints of such a structure are not supported by other data.

3.2.2 Reduction to the pole

Unlike gravity anomalies that are primarily located over their causative bodies, magnetic anomalies are dependent upon their directions of magnetization and on the direction of the earth's regional field. Reduction to the pole filtering removes the directional dependency and transforms an anomaly into the one that would be observed with vertical magnetization. As

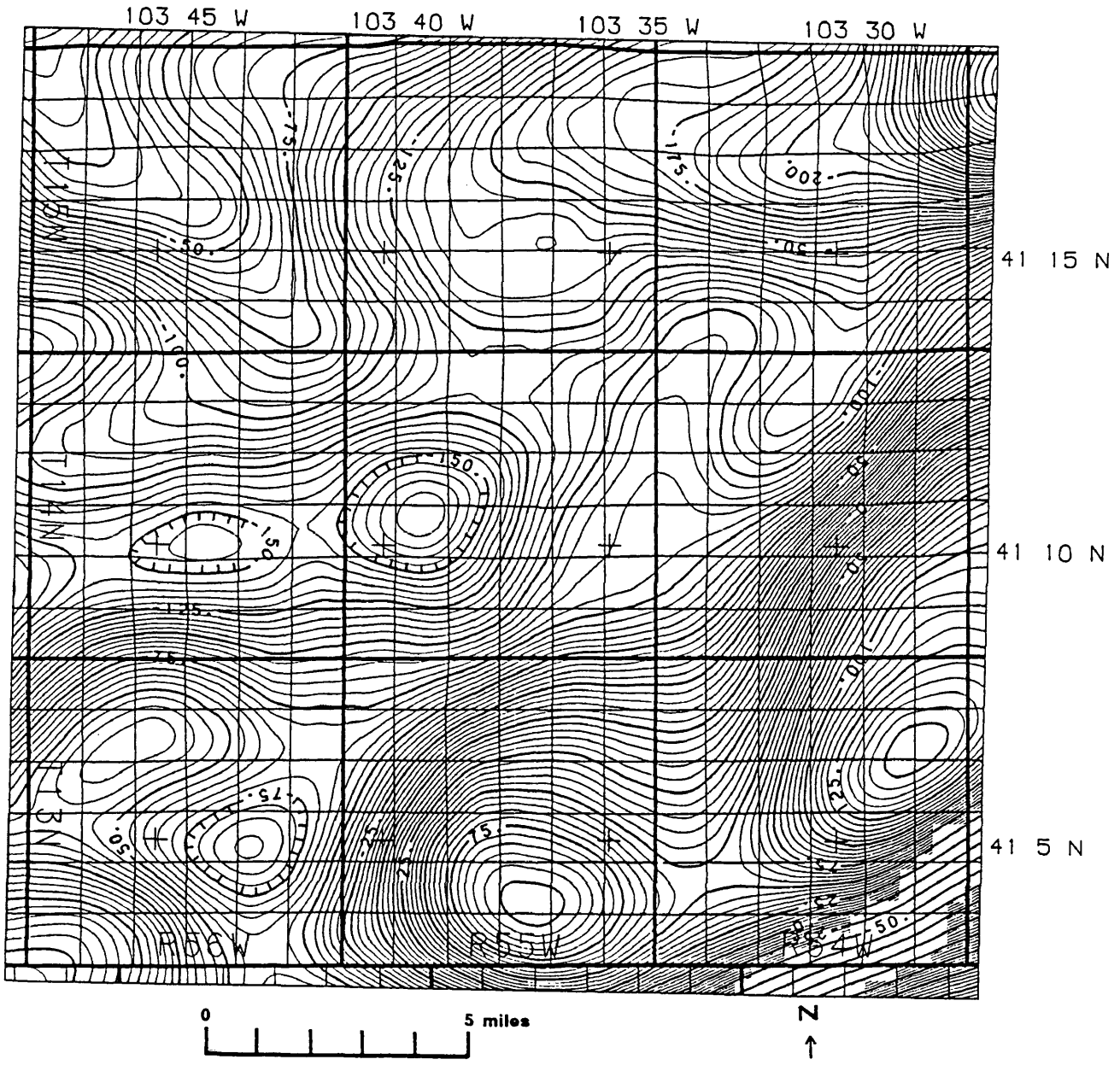

Figure 3.2 Total magnetic intensity, IGRF removed
(Contour interval = 5 nT)

magnetization and moves the anomalies to a position more directly over their causative bodies, thus facilitating the integration of geologic and other geophysical data with the magnetic dataset (Figure 3.3). The reduction to the pole operator can shift the larger magnetic responses northwards as much as several miles. Additionally, linear features and contacts are better defined. For this study, the earth's principal magnetic elements that are accounted for in the reduction to pole filter are:

Total Intensity:	57,000 gammas
Declination:	12° east of north
Inclination:	69° down to the north

The reduced to pole magnetic map shows both strong northeasterly and northwesterly trends in accordance with regional geology. Because of the large amplitude variation along the northeast trend, the anomaly in the southeastern quarter of the study area must be partially, if not completely, due to a lithologic variation in the Precambrian. Since wells are infrequently drilled to Precambrian and are rarely cored, it is not possible to determine this exactly. Wells to the south that are drilled into Precambrian penetrate into horneblende-plagioclase gneisses (Edwards, 1963). These areas have a low magnetic response. Within the higher magnetic response areas, no cores or cuttings are known to exist. A strong northwesterly trend is also represented in the reduced to pole dataset. The more subdued response indicates either a more subtle lithologic change, the presence of structures on the

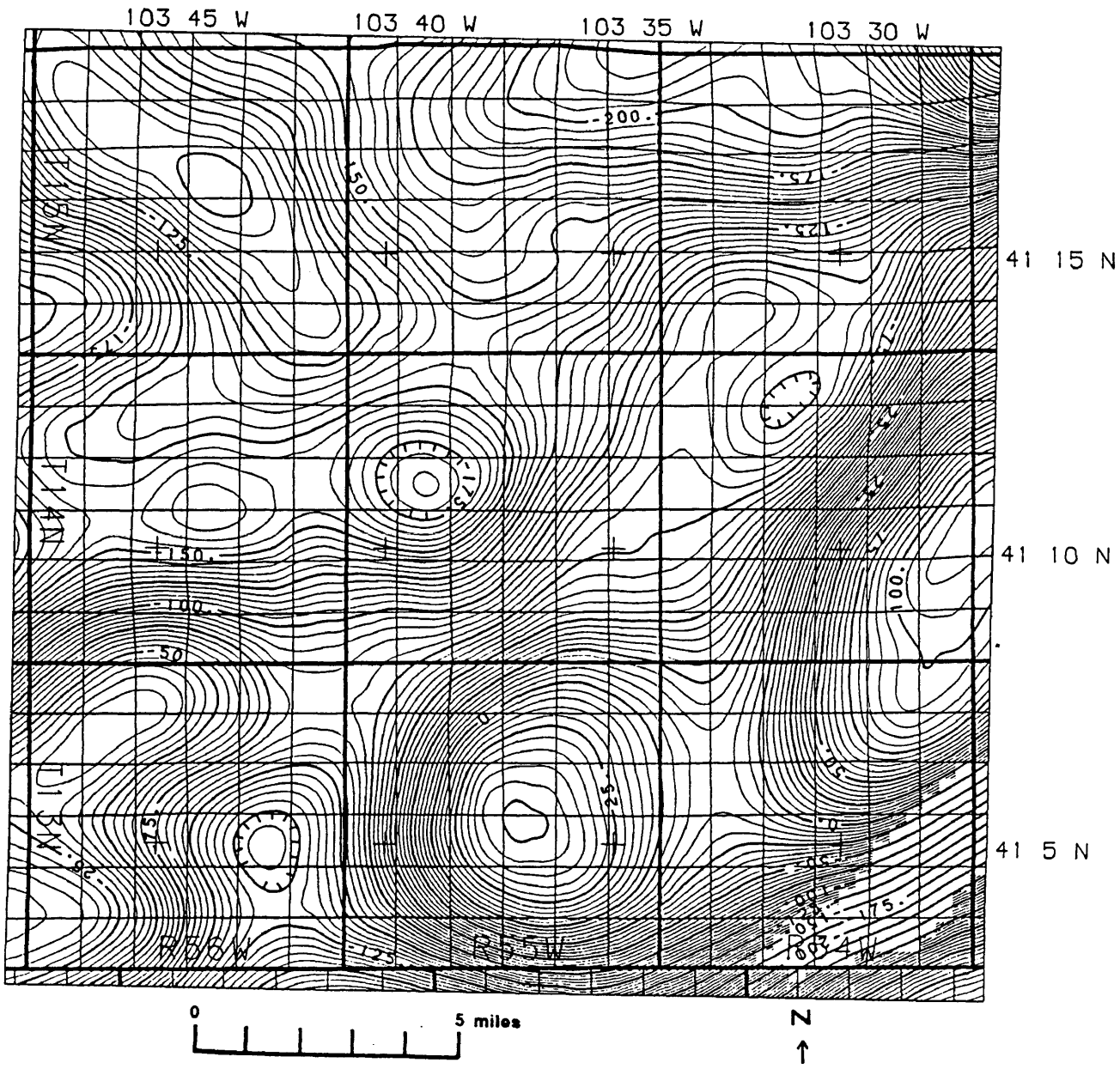

Figure 3.3 Total magnetic intensity, reduced to the pole, IGRF removed (Contour interval = 5 nT)

Precambrian surface, or a combination of both.

3.2.3 Horizontal gradient map

After the reduction to pole correction, a magnetic body is spatially directly associated with the related magnetic response, and the maximum gradient of the anomaly slope is located near or over the body edge. Figure 3.4 shows a west to east profile over a theoretical magnetic body edge. The magnetic anomaly trace shows a magnetic high on the positive side of the block and a low on the negative downthrown side. A horizontal gradient operator computes the absolute value of the slope of the magnetic curve. The maximum of the horizontal gradient curve appears over the contact. That is, the horizontal gradient operator produces maximum ridges on a map over edges of magnetic basement blocks and faults. In addition, the horizontal gradient highlights linear features, related to linear contacts, in the data set. The horizontal gradient map of the reduced to pole magnetics is presented as a contour map (Figure 3.5).

To further enhance the horizontal derivative display, a series of shaded relief maps (shadowgraphs) were generated. The shadowgraph is a display technique that better exhibits the full dynamic range of the horizontal gradient data. Shadowgraphs of aeromagnetic data are produced by near photographic imaging of a digital grid. By assigning gray-scales to the reflectance as a function of data gradient, a shaded relief image is produced. The magnetic

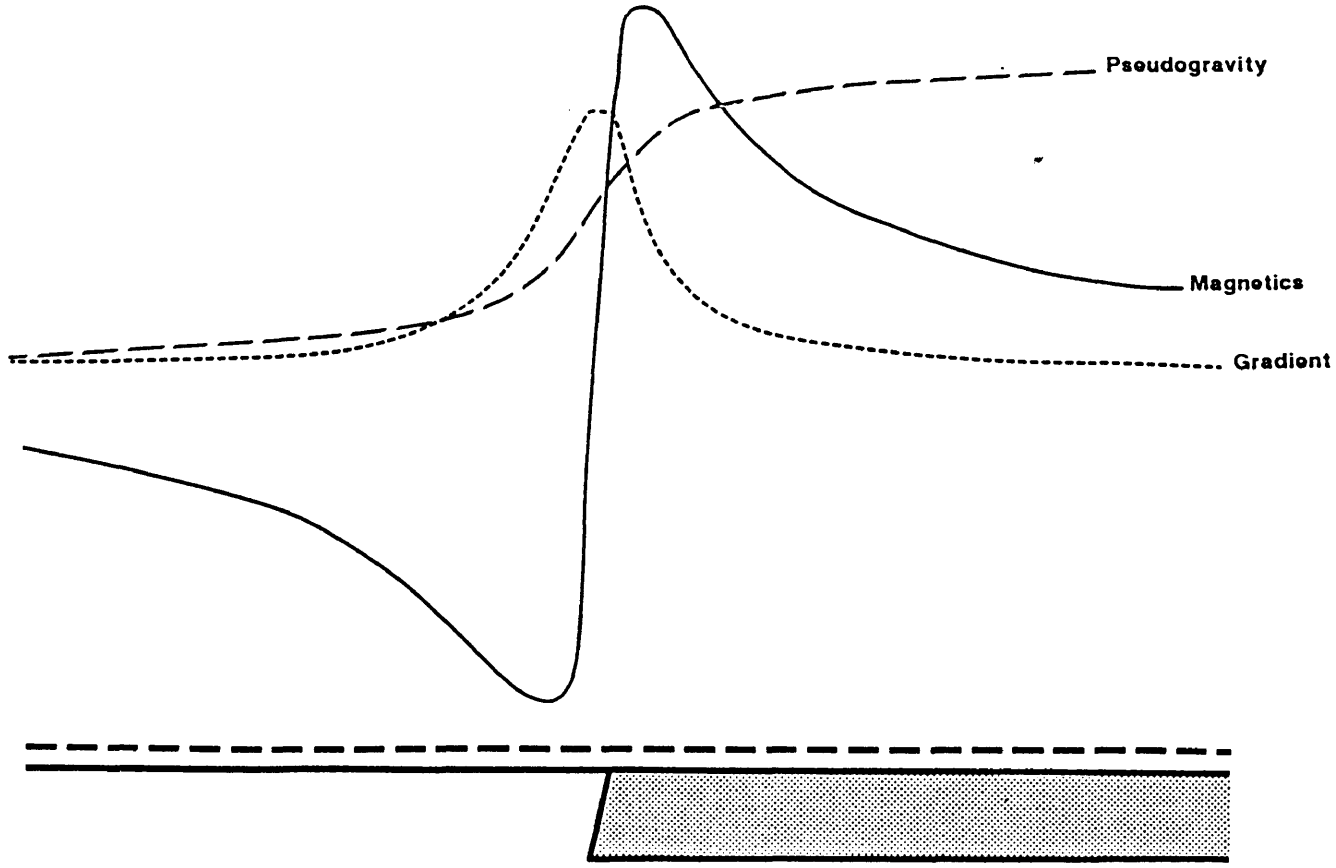

Hypothetical two-dimensional steep contact, showing the observed magnetic anomaly $t(x)$, its pseudogravity counterpart $g(x)$, and the magnitude of the horizontal gradient of the pseudo-gravity $|\partial/\partial x\ g(x)|$. Inclination = 60 degrees; declination = 0 degrees. Units are arbitrary.

Figure 3.4 Horizontal gradient operator (from Cordell and Grauch, 1985)

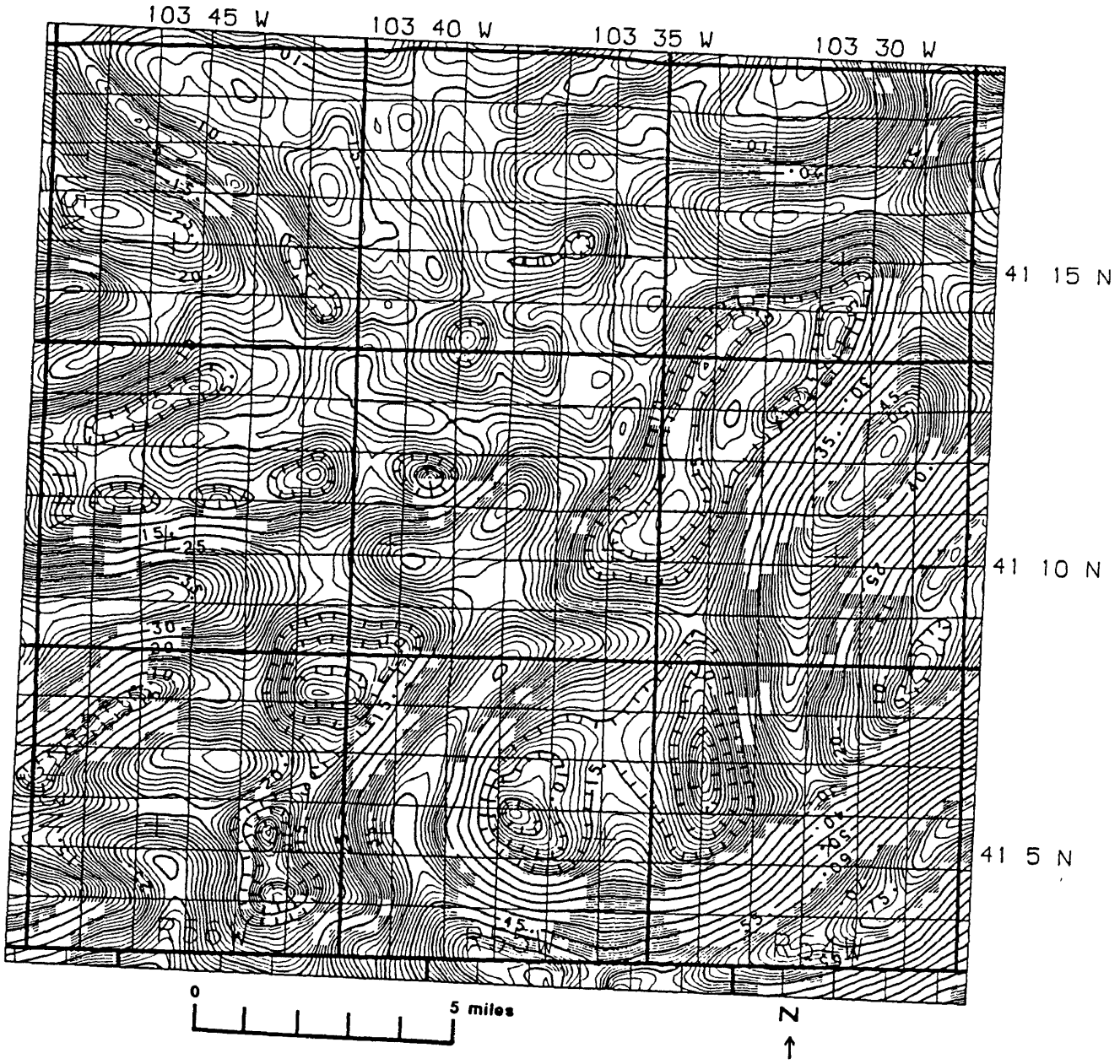

Figure 3.5 Horizontal gradient of reduced to pole magnetics
(Contour interval = 1 nT/ 500 m)

field is treated as a topographic surface and the reflectance of a synthetic sun's illumination from that surface calculated. Hence, horizontal gradient maxima and minima appear as ridges and valleys respectively. Additional, subtle variations, which are difficult to see in a horizontal gradient contour map, are easily visible in a shadowgraph. By examining several different synthetic sun angles, features trending in various directions can be delineated. An example of a shaded relief image of the horizontal gradient of the reduced to pole magnetics (synthetic sun from the northwest) is given in Figure 3.6. Again, the strong northeasterly trend of the data is readily visible. These maps, however, highlight the bending of this trend to a more northerly trend at the area where the northwest trending feature intersects it. This indicates that the northwesterly trending feature is of younger age than the large northeasterly trending one. This also indicates that if there are structures associated with the northeast trend, they are more apt to be localized in the area where the cross-cutting trend occurs.

3.2.4 Second vertical derivative map

To enhance local anomalies and de-emphasize regional anomalies related to intrabasement susceptibility variations, a second vertical derivative of the reduced to pole total magnetic intensity was performed and mapped (Figure 3.7). Mathematically, the second vertical derivative is a measure of the convexity or concavity of the reduced to pole magnetic field. Hence, broad responses from deep within the Precambrian will not have an appreciable response. For example, the high amplitude northeasterly anomaly does not show as a single,

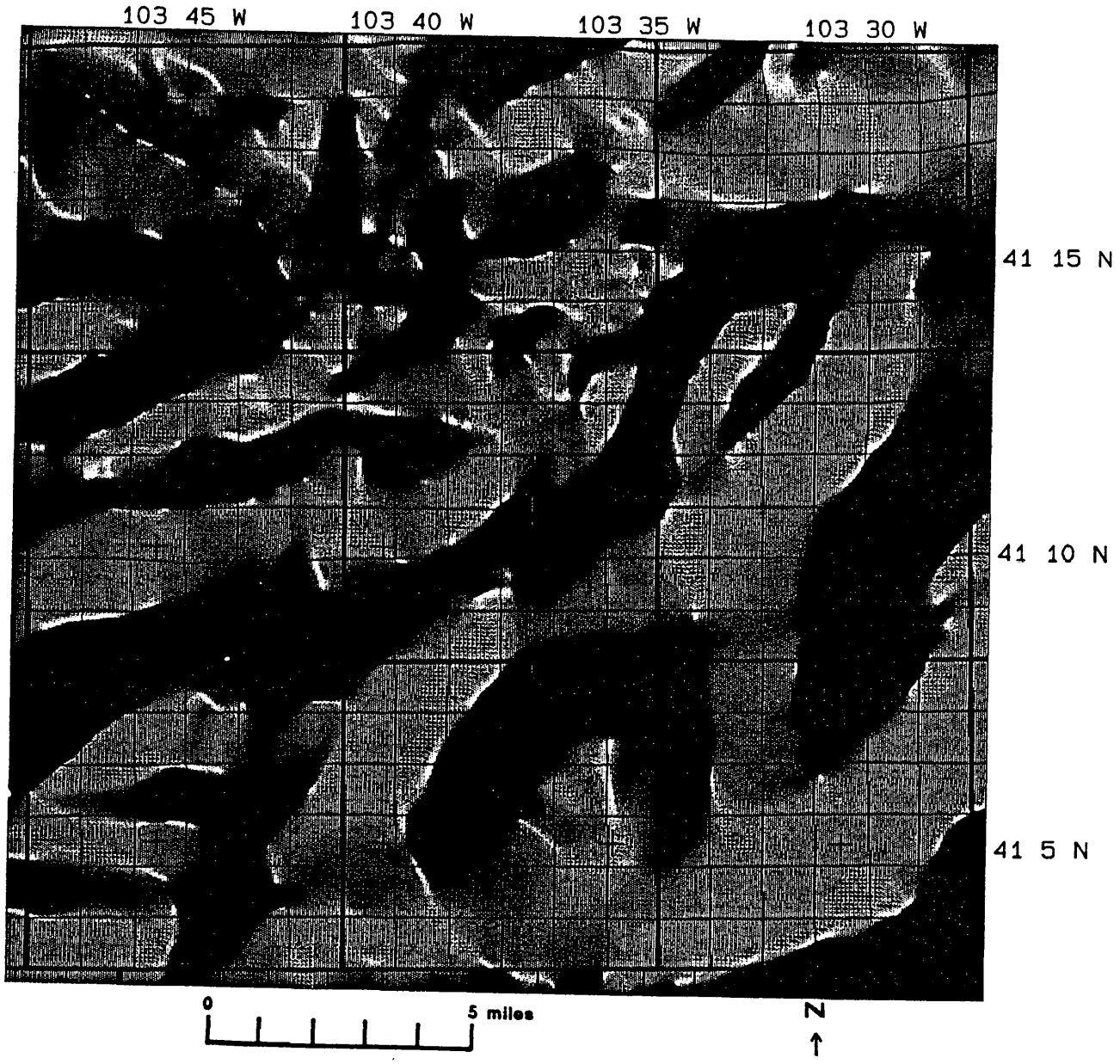

Figure 3.6 Shaded relief image of horizontal gradient of reduced to pole magnetics (White = highest gradients; black = lowest gradients)

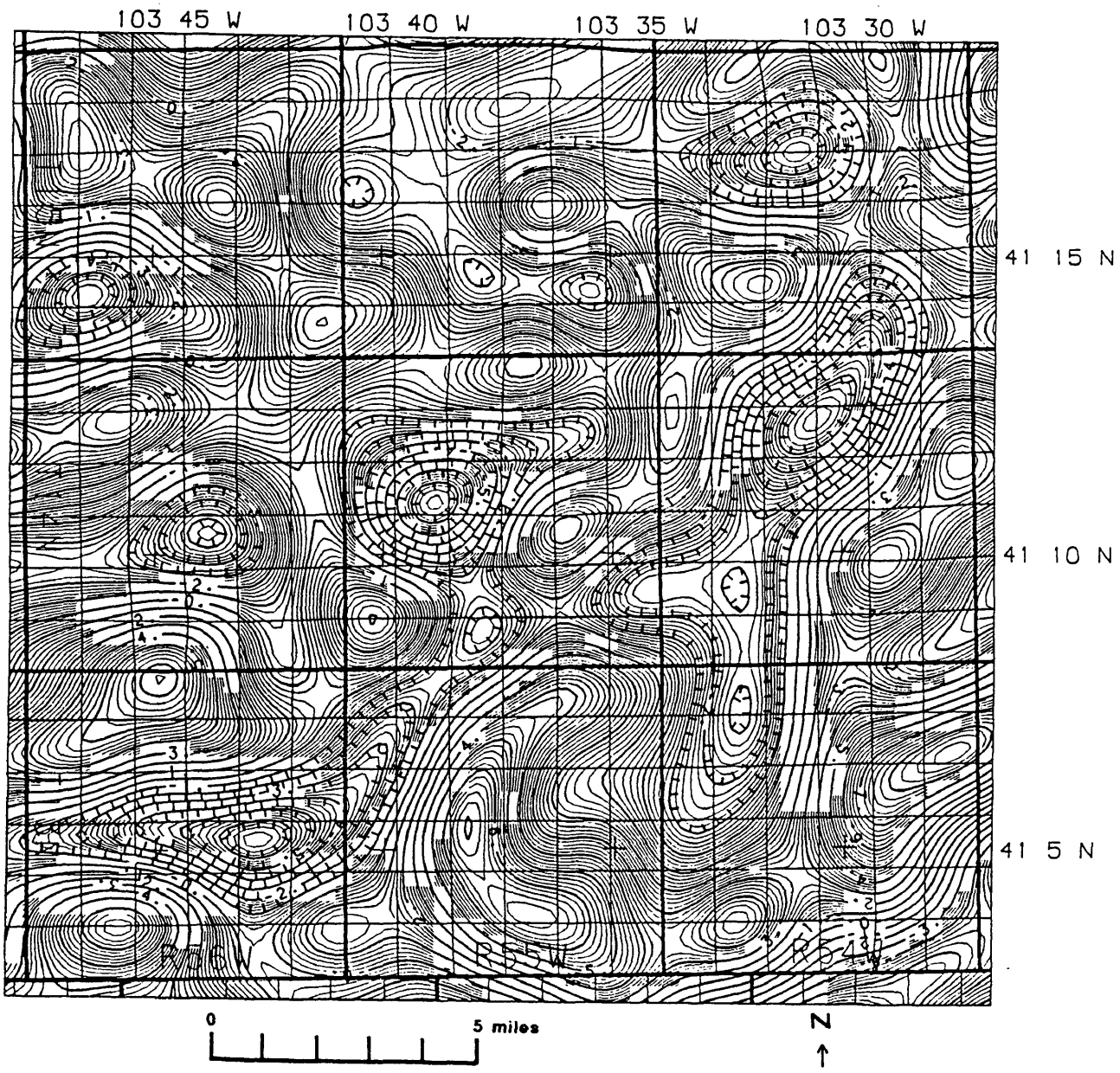

Figure 3.7 Second vertical derivative of reduced to pole magnetics (Contour interval = .2 nT/ 500 m²)

continuous feature, but has been broken into smaller pieces. From a geologic point of view, this map enhances anomalies of possible structural origin. This display confirms the statement that if there are structures associated with the northeast trending anomaly, it is probably in the area of the intersection with the northwesterly feature. Additionally, high amplitude anomalies are associated with shallower-sourced bodies. With this display, structural detail is more sharply focused and magnetic lineament directions are well delineated. This display thus served as an additional verification of features in the lineament pick map.

3.2.5 Susceptibility inversion

A 3-dimensional susceptibility inversion was completed using the first-order approximation structure map of the top of Precambrian and the reduced to pole map as input data sets. A constant thickness of 10,000 meters below the top of Precambrian was used to represent the upper part of the Precambrian section. The resulting susceptibility map (Figure 3.8) indicates the broad susceptibility variations that are required within the upper Precambrian section to satisfy the regional features of the magnetic field, corrected for the variable depth of basement. As the susceptibility determined as such is a contrast, rather than an absolute value, calculated values range between 850 micro cgs-units and 1350 microcgs-units. It must be realized that the relative values of the determined susceptibilities can be changed by changing the thickness of the plate used in the inversion, but it is considered that the upper 10,000 meters of the Precambrian section probably represents the main part of the magnetic

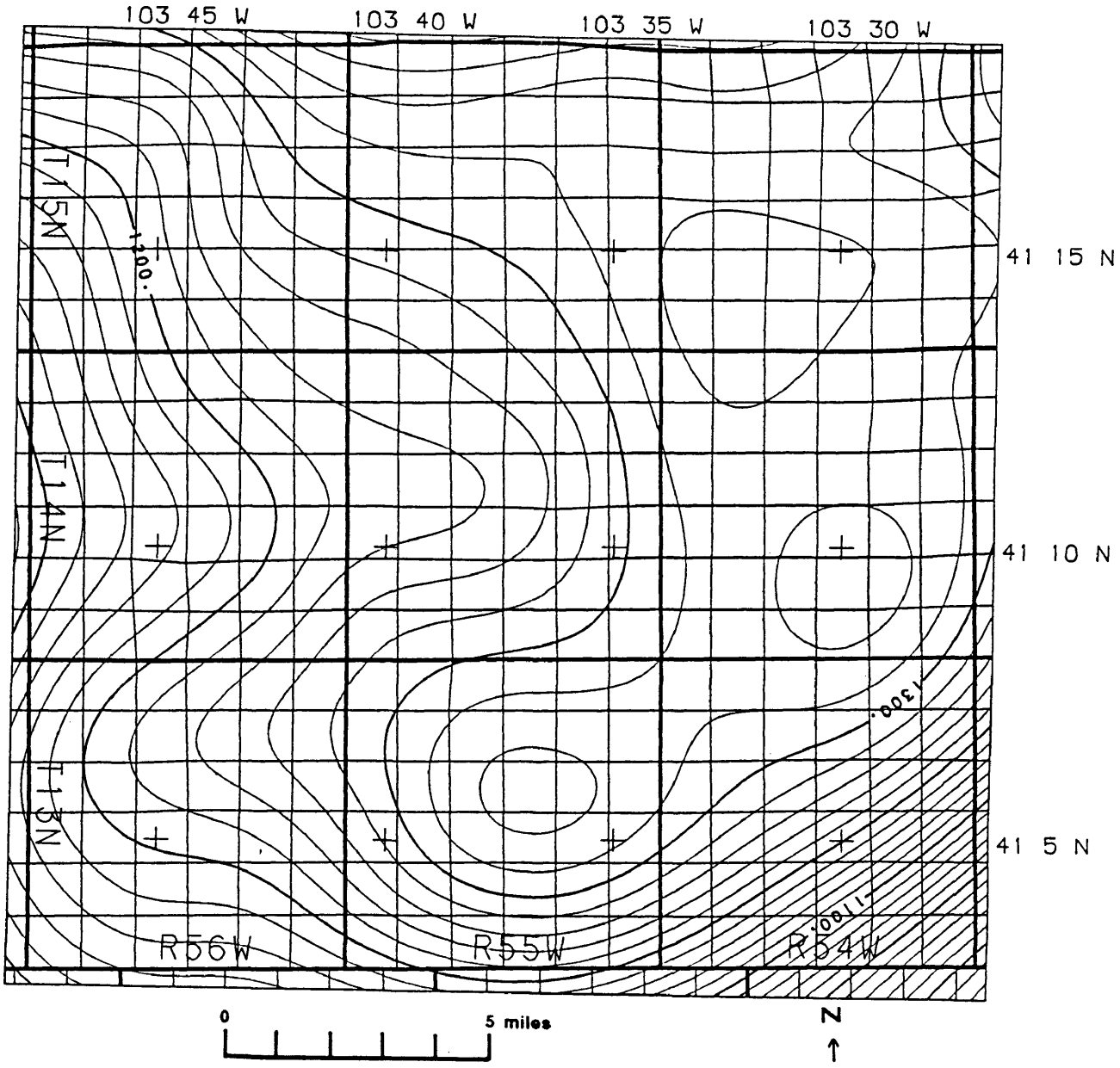

Figure 3.8 Susceptibility inversion
(Contour interval = 20 µcgs units)

field associated with basement. It is nevertheless clear that significant lithology differences are present within the assumed Precambrian basement section.

3.2.6. Forward magnetic models

The magnetic field from the first-order approximation of Precambrian was calculated and mapped using both the determined susceptibility grid, as well as a constant susceptibility of 1,000 μcgs-units. All forward calculations were completed using vertical magnetization, to facilitate comparison with the reduction to pole map. By using the variable susceptibility grid as an input, this model should satisfy the major, regional magnetic responses observed on the data sets, with differences in the amplitudes of the anomalies accounted for by the broad, regional variations in the susceptibility grid. Figure 3.9 shows that the broad, regional northeast trending magnetic high in the southeastern quarter of the survey is reasonably well represented in the calculated model, and is considered related to the combination of overall basin shape and inferred basement lithology. The primary difference is the large northwest trending anomaly in the northwestern quarter of the data set. This feature is not represented in the regional, basement-lithology related forward model.

Next, a forward calculation using a constant susceptibility was performed (Figure 3.10). As the determined susceptibility variations are large, and some of the smaller structures in the low susceptibility zones may not be easily discerned, the forward calculation was repeated using a constant susceptibility of 1,000 μcgs units. This process enhances the

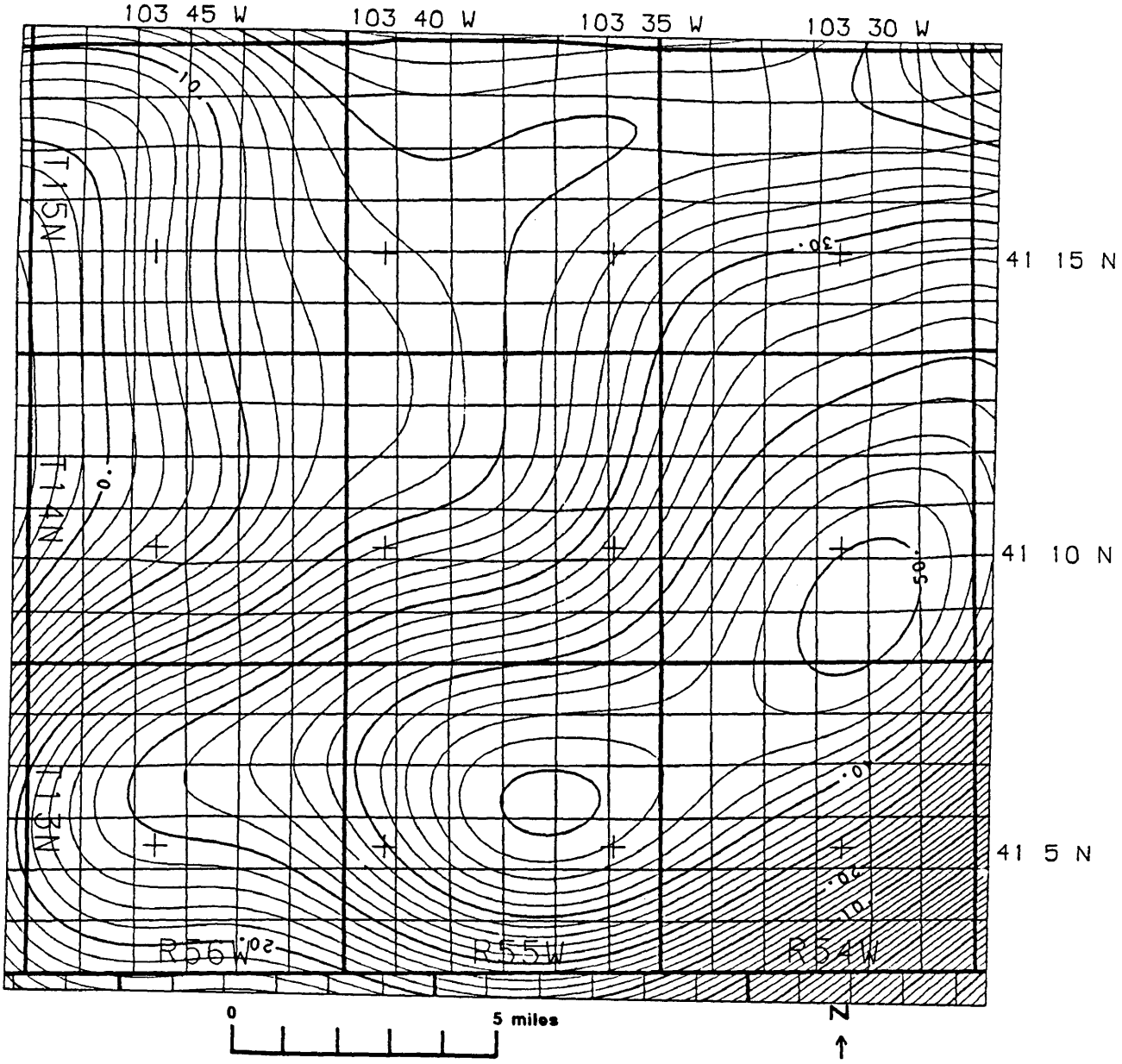

Figure 3.9 Forward magnetic model using susceptibility grid (Contour interval = 2 nT)

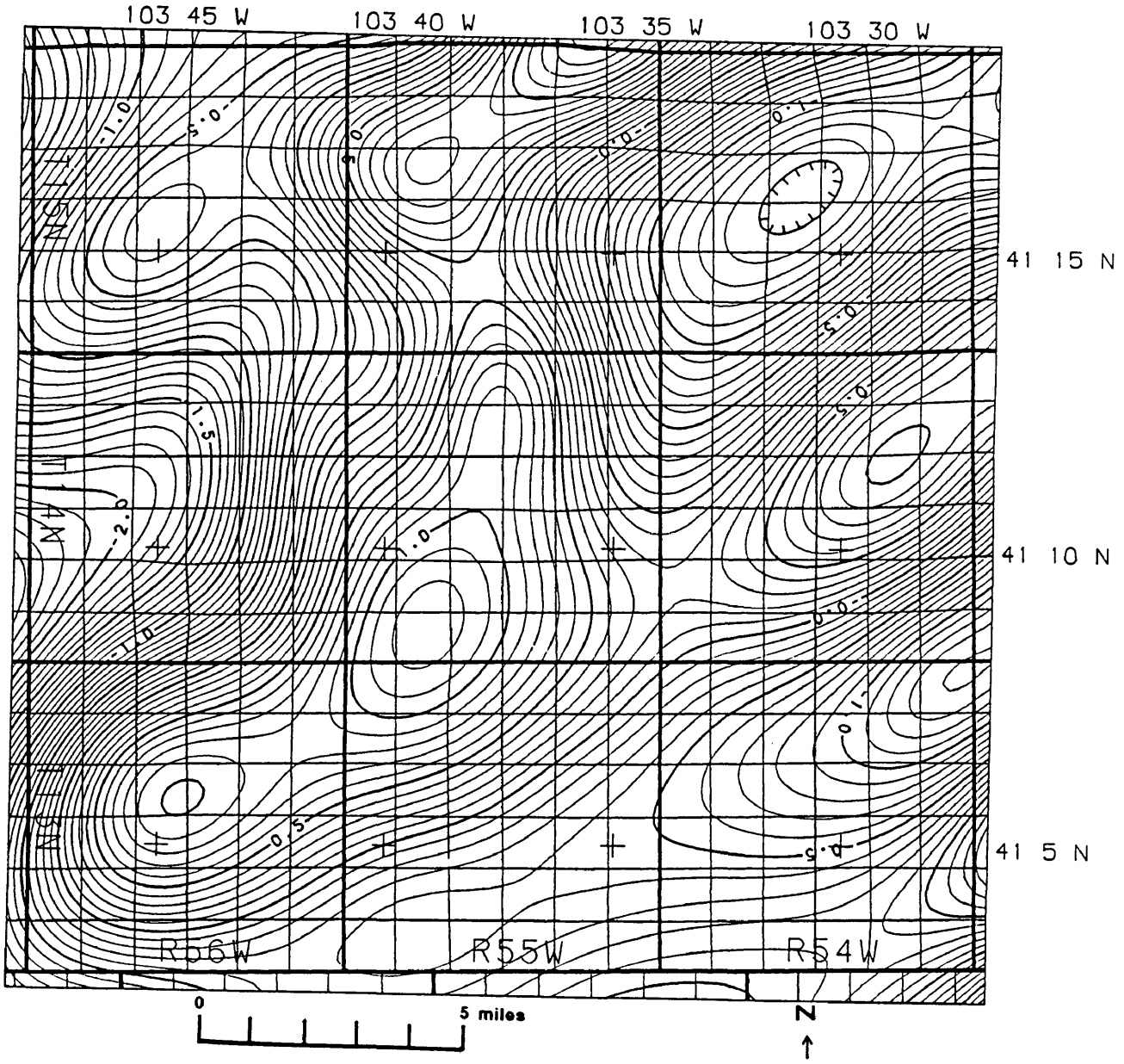

Figure 3.10 Forward magnetic model with constant susceptibility (Contour interval = 0.1 nT)

anomalies associated with basement structures and the shallower parts of the basin. All the calculated anomalies are very small in amplitude, a few gammas or less, and indicate the range of responses that could be associated with known geologic structures. Although the northwest trending feature is not well represented in this display, the northeastern flank of it is. This indicates that the anomaly is probably a subtle lithologic change with associated structure primarily along this northeastern edge. In the southeast, the broad lithologic anomaly possesses a series of small responses that are aligned along an axis oriented parallel to it. This leads to the confirmation that should structures be associated with this feature, they will be along the flanks.

It should be noted that the two forward models have isolated the two principal components of the magnetic field. The first model represents the low-frequency, high-amplitude susceptibility portion of the field, while the second represents the high-frequency, low-amplitude structural portion. These two models, therefore, can be considered the products of a process that is analogous to regional/residual separation in gravity prospecting.

The manual analysis of all of these datasets requires significant time and experience. For a small study area, this is not a limiting constraint. As the area of investigation increases and the geology becomes more complex, the isolation and identification of each individual anomaly becomes more difficult, more time consuming and, therefore, more costly. For the analysis of a large survey, automation of this process would be an invaluable aid.

Chapter 4

TWO-DIMENSIONAL DATA ANALYSIS

4.1 Introduction

Two-dimensional data analysis is in several ways superior to three-dimensional map analysis. For this study, all grids were created using a minimum curvature algorithm (Webring, 1981). Regardless of which gridding algorithm is used, however, some degree of data smoothing is inherent. Thus, extremely subtle anomalies may be completely eliminated just by mapping the data. Also, when using one of the various two-dimensional methods, the actual profile data as acquired in the field can be used. There are several profile analysis techniques that are available to the engineer. These include Euler deconvolution, Werner deconvolution, and forward and inverse modeling (Blakely, 1995). All of these methods, however, have one characteristic in common---they are time consuming and labor-intensive interpretation methods. By utilizing the power of artificial intelligence, an alternative automated method has been developed using neural networks.

4.2 Fundamentals of neural networks

A neural network is a computational system that utilizes organizational principles similar to the biological network of the human brain (Rogers et. al., 1992). That is, a neural network

is a fundamentally different alternative to sequential, conventional programming. Conventional programming in a structured language (e.g. FORTRAN, BASIC, C) is a sequential execution of user-defined commands for the solution of a problem. From beginning to program completion, a linear flow of command is executed, with data stored in discrete addresses. In contrast, a neural network is not a series of programmed commands that searches memory locations for operations and data. Rather, neural networks are massively parallel systems of simple interconnected units that respond collectively to external inputs. Knowledge is distributed throughout the individual nodes and their interconnections (Rumelhart, et. al.,1986). A neural programmer does not give commands to execute, but, rather, defines network parameters such as the number of processing nodes, the interconnection of the nodes, and the rules for learning. In general terms, a neural network does not execute programs; rather, it reacts similarly to the human brain (Caudill, 1987).

4.3 Biological analogy of neural computing

Since neural networks operate similarly to the way the human brain is presumed to work, it is natural that their structures are analogous. The human brain is a complex organ that consists of billions of cells called neurons. An individual neuron has input connections called dendrites, a central nucleus that weights and sums signals that are passed to it through the dendrites, and output connections to other neurons called axons (Figure 4.1). Each neuron typically has between 1,000 and 10,000 connections. As different inputs enter the paths to

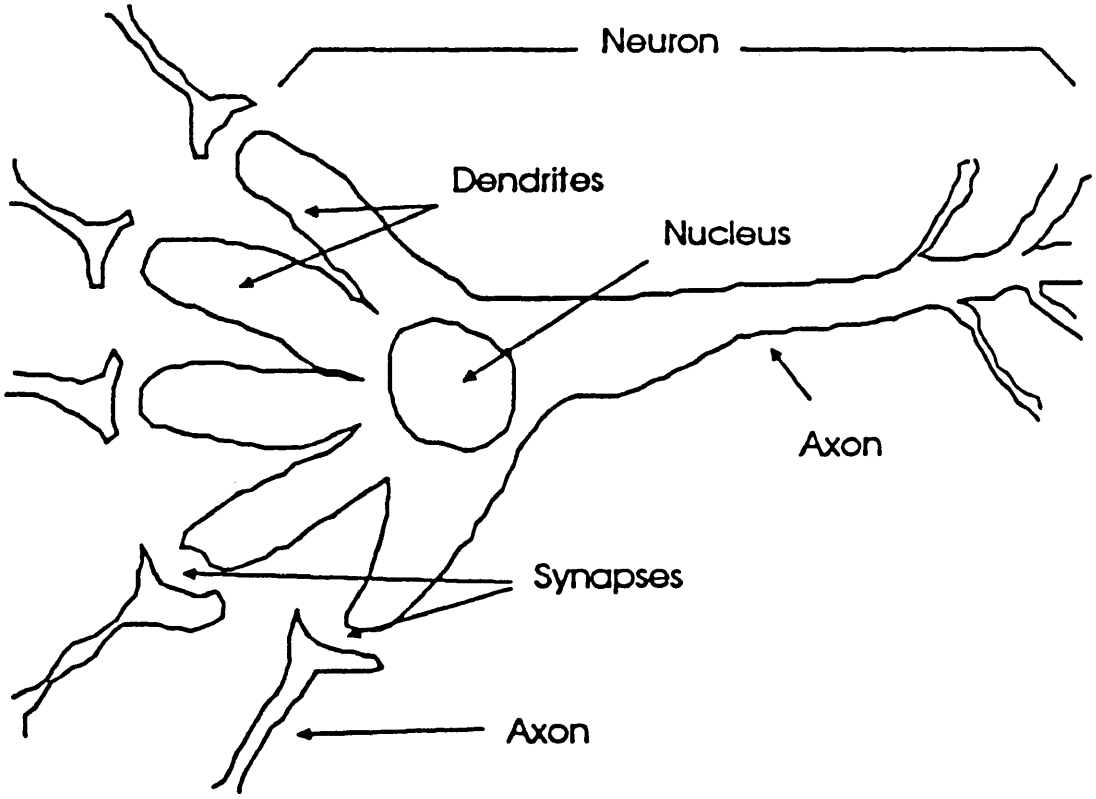

Figure 4.1 Biological neuron
(reprinted with permission of NeuralWare, Inc.)

an individual neuron, the brain formulates a response. Depending upon the set of inputs, the individual neuron may either fire or not fire. The response to fire or not fire from the brain is a combination of both genetics and acquired learning (Nelson and Illingworth, 1991).

By analogy, a neural network is a collection of simple, interconnected units called processing elements. Each processing element is composed of input paths, a central node that sums input signals and determines whether a firing threshold has been attained, and output paths which connect with other processing elements in either the same or adjacent layers (Figure 4.2). In neural networks, there is no innate knowledge. At the beginning of training, all connecting weights between processing elements are set by a random number generator. All of the connection weights are learned during training. As in the human brain, individual neurons are not the storage locations for information. Knowledge is not localized into memory addresses; it is spread throughout the collective system of thousands of processing elements and their interconnections (Nelson and Illingworth, 1991).

4.4 Neural network paradigms and their uses

Neural networks have a great variety of applications including predictive modeling, signal processing, and pattern recognition. Because of the diversity of present applications, a significant amount of research has been done in advancing the science to the present state. Guo (1992) gives a brief treatment of neural network history and applications. Within the oil and gas industry, neural networks have been used to pick first breaks and trace horizons in

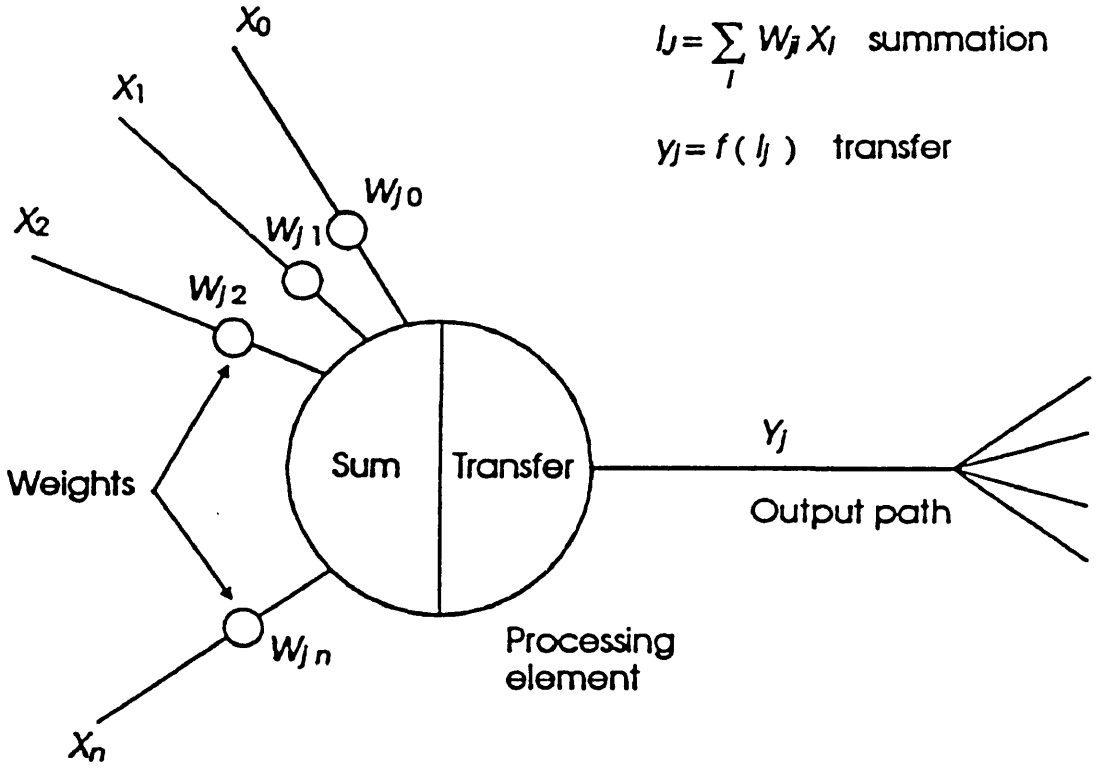

Figure 4.2 Neural network processing element
(reprinted with permission of NeuralWare, Inc.)

seismic studies, interpret gas chromatographs, interpret well logs, generate logs for incomplete suites, and detect fractures from high resolution well-bore images (Veezinathan, 1991).

At the present time, there is a great variety of neural architectures available to the operator. Table 4.1 is a brief summary of these paradigms. Many of the paradigms are unable to learn non-linear, hetero-associative tasks. For example, the Perceptron network has difficulty handling problems that are not linearly separable. Similarly, the bi-directional associative memory (BAM) and Brain-State-in-a-Box (BSB) models work well with auto-associative data, but poorly, if at all, with hetero-associative data. As a result, choosing a neural network paradigm is dependent upon the type of problem that is to be solved. For this study, several different architectures were examined. These included the Boltzman machine, counter propagation, and back propagation. Although it could solve the problem, the Boltzman machine displayed several undesirable characteristics including an inordinately long training time and great difficulty with noisy data.

Similarly, although the counter propagation network would sometimes converge, if two examples with very similar inputs produced different outputs, the network oscillated rapidly and failed to recognize the differences. Although both of these problems also existed in the back propagation network, they occurred at a significantly lower rate. Additionally, since the back propagation paradigm is the architecture most commonly used and probably the most easily learned, it was settled upon as the model to be used.

- Adaline and Madaline
- Adaptive Resonance Theory (ART)
- Back propagation
- Bi-Directional Associative Memory (BAM) networks
- Boltzmann Machine
- Brain-State-in-a-Box (BSB)
- Cascade Correlation Networks
- Counter propagation
- Delta-Bar-Delta Networks
- Directed Random Search Networks
- Hopfield Networks
- Kohonen Feature Map Networks
- Neocognitron
- Perceptron Networks
- Recirculation Networks

Table 4.1 Neural network paradigms (after Nelson and Illingworth, 1991)

4.5 Back propagation networks

As previously stated, back propagation networks are the most popular networks in use today. The term back propagation is in reference to the manner that the system handles errors. The back propagation algorithm is firmly based in mathematics and, therefore, is easily understood. Although this model has no resemblance to the processing of information in the human brain, it is still highly effective.

Back propagation networks always are composed of at least three layers. The first, or input layer, is an externally connected set of processing elements to which the user presents data. Similarly, an external output layer returns data to the user from the network. At least one, possibly more, internal or hidden layers are also present. Figure 4.3 is a schematic of a back propagation network with one hidden layer.

The back propagation network involves supervised learning. That is, both input responses and their corresponding outputs are given to the network. The network reads in an input and passes forward the information to the output layer. Since all processing elements are connected to all other processing elements in the adjacent layers and since all initial connection weights are random, the output that the network calculates will probably be very different from the actual output. The network calculates the magnitude of the error and assumes that all connections to the output are partially responsible for the discrepancy. The connective weights are then adjusted to decrease the magnitude of the error. After updating the connection weights, another input/output pair is presented, and the process is repeated.

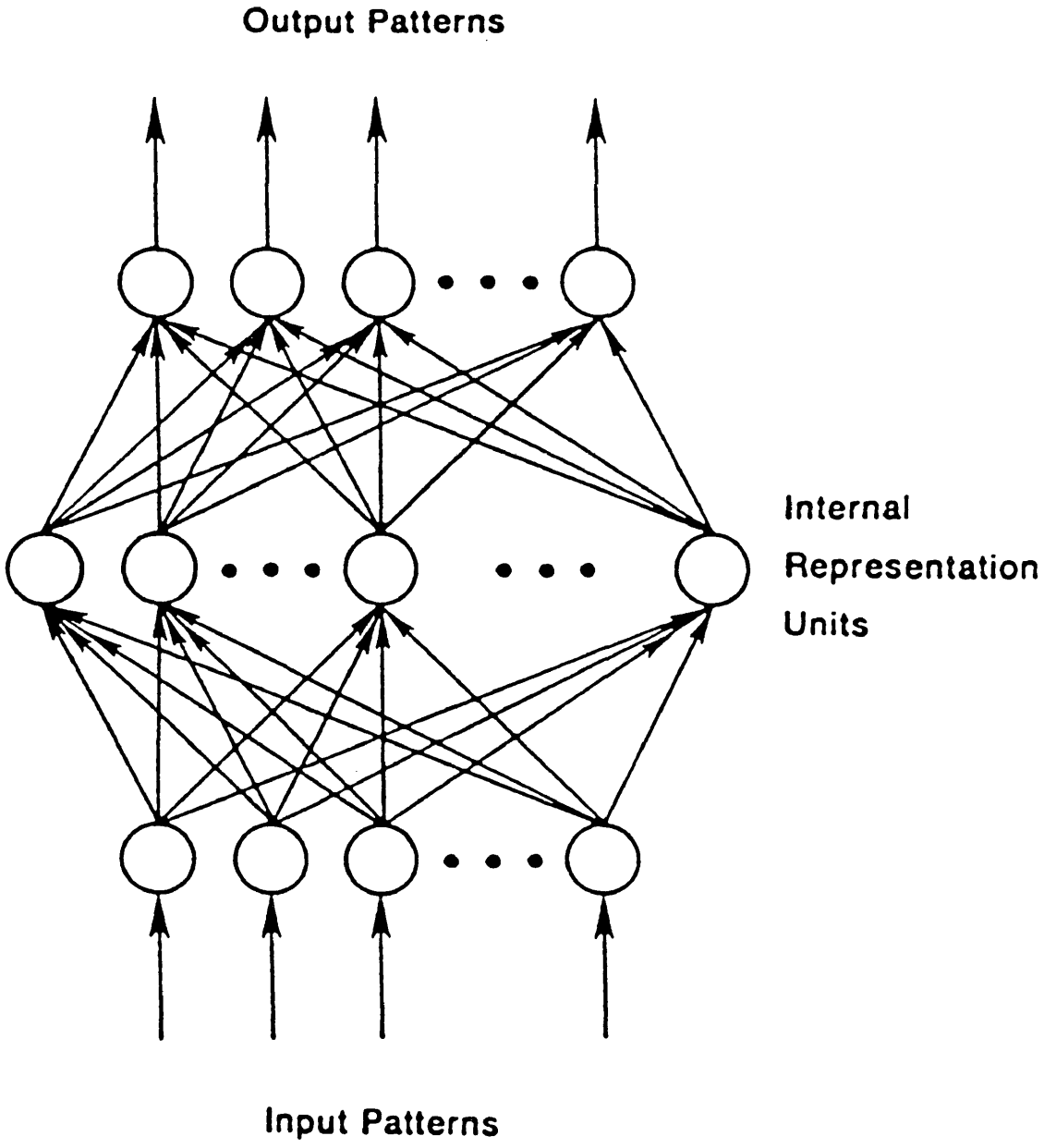

Figure 4.3 Three layer back propagation network architecture (from Nelson and Illingworth, 1986)

When the difference between network-generated and actual outputs reach a user-defined convergence criterion, the network is tested on more examples that were not used in the training stage. If the two outputs are very similar, then the network has been trained and is ready to run on actual field data. Rumelhart et. al. (1986) provide a discussion of the mathematical basis for the back propagation learning mechanism, called the Delta Rule.

4.6 Neural network output and comparison with three-dimensional analysis

For this study in the panhandle of Nebraska, a three-layer back propagation network was trained to recognize the location, width, and amplitude of structures on top of the Precambrian surface. General neural architecture parameters are available in Moll et al. (1994). The neural network was created using the commercially available product NeuralWare, version 4.0. Additionally, susceptibility blocks were modeled to train the network to discern between structural and lithologic magnetic responses. Following previous work by Pearson, Wiener, and Moll (1990), the network was trained on both synthetic and real data. The synthetic data were created by examination of public domain seismic information (Montgomery, 1987). Synthetic basement structures were created and added to the low-pass basement surface. Forward magnetic models of these features were then generated and data windows discretely sampled. Target size parameters determine the number of input nodes. Building upon and following similar procedures done in work by Moll et al. (1994), twenty-one input nodes (profile sample points) were used to represent a

window of the aeromagnetic data. Twenty-one fully connected nodes in the hidden layer were connected to one single output node. The output of the neural network on profiles is a residual structural anomaly amplitude. Selectively edited for spurious anomalies, the data are subsequently gridded up (Figure 4.4), and added to the low-pass version of Precambrian structure found in literature (Montgomery, 1987).

A comparison of the neural network results with the second vertical derivative map (Figure 3.7) shows that the conventional map analysis yields many more anomalies than the two-dimensional interpretation. In a small area such as this, the analysis of all of the second vertical derivative anomalies may take no more time than the training and operation of the neural network. However, as the study area grows larger, the time and cost differential between manual and automatic interpretation methods grows significantly larger. Additionally, the second vertical derivative map does not directly show information about the amount of relief associated with structural anomalies. An additional step is associated with the manual analysis as compared with the neural network results which indicate not only the size of structures, but also the depth to them at the time of output. Hence, the two-dimensional analysis has the effect of performing the map analysis and subsequently high grading it.

It should be noted that a statistical analysis for measuring the sensitivity of the results was not undertaken for this work. Most neural networks are unable to provide a measure of the certainty of the predicted results (Weiss and Kulikowski, 1991). A number of methods for

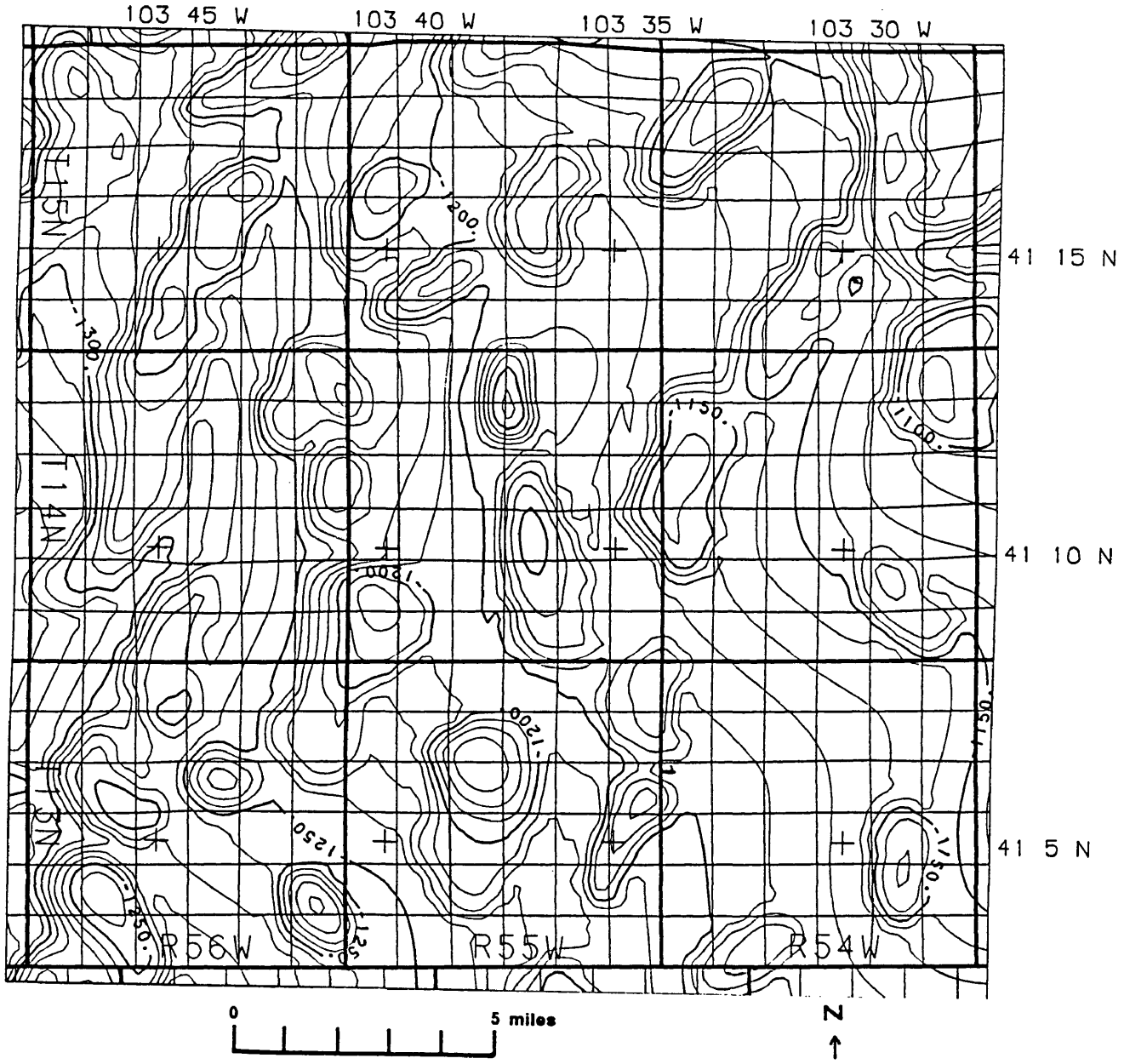

Figure 4.4 Neural network output---depth to Precambrian basement (Contour interval = 10 meters, datum is sea level)

solving this shortcoming are currently being examined. These statistical approaches include cross validation (Weiss and Kapouleas, 1989), cross entropy (Hertz et al., 1991), probabilistic neural networks (Specht, 1990), bootstrapping methods (Efron and Tibshirani, 1993), and active learning (Cohn et al., 1995).

Chapter 5

DISCUSSION AND CONCLUSIONS

5.1 Hydrocarbon production in the Nebraska Panhandle

Several fields consisting of more than one well have been developed in the Paleozoic strata within the study area. In all, 56 wells have produced a total of over 5,000,000 BO, and 1,500,000 MCFG from the Upper Paleozoic in the study area, as of January, 1996 (personal communication, Nebraska Oil and Gas Commission). Kleinholz, Terrestrial and Bird fields are responsible for the bulk of this production.

In 1986, the Exxon discovery of oil in the Lower Wolfcamp (1 James Koenig in 17-14N-56W) extended known production to Paleozoic horizons into Kimball County (Sahl et al., 1993). Subsequent development has resulted in the completion of 27 wells to the northeast creating Kleinholz field. Production is from the Admire A, B, and C zones (originally completed in the discovery well) and from the Permian Wykert sand. Perforated in the Koenig No. 2., Wykert production has outstripped production from the Admire, leading many operators to opt to produce from the highly productive and laterally continuous Wykert, and subsequently leaving the Admire behind pipe for future completion. This strategy is intended to avoid drainage by neighboring leases (Hart, 1992). The Wykert produced 340 BOPD in the Wykert No. 1 well, with no water (pers. comm., John Webb). Very little water

has been produced from the Wykert Sand. Gas is produced at some wells, with IPs as high as 102 MCFGPD. The completion of the Advantage Gross Bros. No. 1 documented the stratigraphic component of the trapping mechanism at Kleinholz. The field occurs on the flank of a second vertical derivative. The neural network shows a structural nose that trends north-northeast (Figure 5.1). Production also occurs in the adjacent low to the east. If the neural network results are correct, Kleinholz field could be extended by several more sections. Sixteen wells were drilled in succession with the field limit yet to be encountered to the northeast. Cumulative production for the 29 wells is 2,495,300 BO, and 1,211,500 MCFG, and includes commingled production from the Admire A, B, and C zones. Water production (from Admire completions) is 160,800 BW.

Anna Field contains three producing wells. Both the second vertical derivative and neural network outputs indicate that Anna Field sits on a structure (Figure 5.1). Production is from the Admire, with cumulative production of 193,700 BO, 15,100 MCFG, and 17,900 BW (Nebraska Oil and Gas Commission, 1996). A cored interval in the Upper Virgil in the Prairie State well encountered highly porous, sucrosic dolomite, with some oil stain.

Swearingen Field was discovered in the 1950's. Extensive production from the Cretaceous "J" sand accounts for almost 95% of the discovered oil. Only in the last six years has production been deepened. While the second vertical derivative shows that the field sits on the flank of an anomaly, the neural network places the field on a structure with almost 200 feet of closure (Figure 5.1). Seismic data over the field have since confirmed this. The field

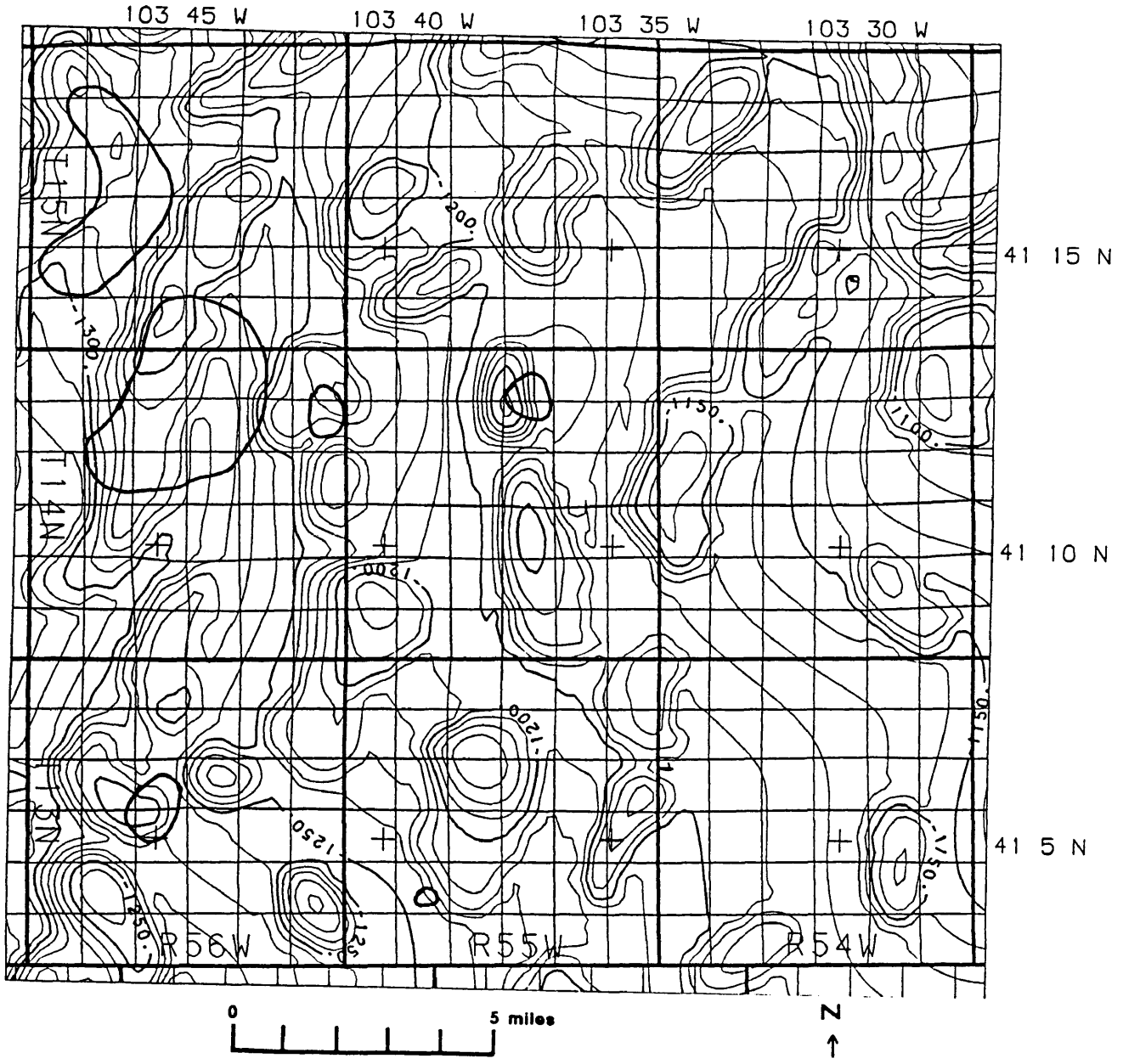

Figure 5.1 Comparison of neural network results with known oil production

contains two producing wells and has no dry holes. Production is from the Admire and the Missourian B zone. IP of the Gieseking #1 was 132 BO, 90 MCFG, and 57 BWPD (Nebraska Oil and Gas Commission, 1993). This completion was the first in Missourian strata in Kimball County. Cumulative production for two wells is 99,800 BO, 182,800 MCFG, and 55,000 BW.

Terrestrial Field was discovered by Exxon in 1990 (pers. comm., John Webb). The second vertical derivative indicates a strong anomaly, while the results of the neural network indicate that the northwestern arm of this field determines the axis of a structural high. The southwestern arm of the field sits in a neural network low, however (Figure 5.1). To date, the field includes 9 productive wells and is delineated along portions of its southern and western flanks by six dry holes. Cumulative production for the 9 wells is 350,400 BO, 85,100 MCFG, and 158,500 BW (Nebraska Oil and Gas Commision, 1996). Production includes at least 1 well with commingled Admire.

Kimball County contains several single-well fields. The Sun Evertson No. 1 well (12-14N-56W) was completed in the Upper Virgil (Mamoo zone) for 120 BOPD, 58 BWPD, and 40 BWPD. The neural network places this well on a subtle basement high (Figure 5.1). The second vertical derivative shows the field is located on an inflection. Cumulative production at Mamoo Field is 63,505 BO, 7,737 MCFG, and 15,031 BW. An offset (Sun Yung No. 1) was dry. Shows have been reported for the Mamoo zone elsewhere in Kimball County, but have yet to be completed for production (Hart, 1992).

The New London Oil Lukassen No. 1 well (8-15N-56W) opened production in the Wykert sand at Dill Field. IP was 23 BOPD with gas too small to measure. Cumulative production is 31,100 BO with no gas or water (Nebraska Oil and Gas Commission, 1996). During subsequent drilling, Terrestrial Field has merged with Dill. The neural network interprets this field to sit on a low-relief basement structure (Figure 5.1); the second vertical derivative shows that it sits atop a small anomaly.

Hart (1992) reports single well Paleozoic production from 29-13N-55W. This well sits on the flank of a large neural network high (Figure 5.1). No further information about this well is known.

5.2 Conclusions and limitations

High sensitivity aeromagnetic surveying in the D-J Basin can be used to map faults and structures at the top of Precambrian basement. A 300-foot terrain clearance survey conducted with a Cesium vapor magnetometer produced better than one gamma sensitivity along the profiles. An integrated geologic/aeromagnetic interpretation method was followed in utilizing the sparse Precambrian tops and the very detailed magnetic structural analysis to produce the final contoured Precambrian structure map. This map was used to provide shaping of the Precambrian structure contours between wells. The correlation between known production and neural network basement structures is excellent. Of the five oil fields in the study area, three are located atop neural network structures while the other two are

partially located on neural network features.

A good local correlation between Paleozoic isopach thins and Precambrian structures indicates that the same areas of uplift and subsidence prevailed throughout Pennsylvanian and Permian time. General thickening of the Paleozoic interval isopach north and west of the Transcontinental Arch and Morrill County High indicate that both evaporite deposition (restricted circulation) and clastic deposition (infilling) were enhanced in the Alliance Basin during Permian time. Depositional thickening south of the Arch is mostly related to infilling of the Cheyenne County Low. Drilling of local structural blocks throughout the study area may continue to yield commercial oil discoveries. However, this study can also help in mapping larger structures and possibly assist in finding larger scale stratigraphic pinchouts of possibly major hydrocarbon significance.

Potential field interpretations such as aeromagnetic studies to explain observed anomalies caused by subsurface bodies are limited in resolution. As basin depth increases, the ability to differentiate between structural and lithologic anomalies becomes tenuous. The magnetic basement interpretation is believed to be an accurate representation of the actual subsurface geology. However, in magnetic interpretation studies, it is not possible to declare with absolute certainty whether a given observed anomaly is produced by a basement structure or by a change in basement lithology. Large amplitude magnetic anomalies must possess a lithologic component, since the magnitude of structure needed to match the observed anomaly would be inconsistent with geology.

Precambrian basement does not have consistent susceptibility. Basement composition varies from granite to metamorphic gneisses. A basement structural high in an area of lower susceptibility basement, such as a metasediment, will not produce a measurable anomaly. It is, therefore, possible that basement faults and structures exist that are undetected by this study.

Magnetic anomalies have been computed by neural network technology and correlated along the individual flight lines to differentiate between suprabasement and intrabasement sources. For instance, suprabasement anomalies have a lower amplitude and a higher degree of curvature than the intrabasement anomalies. Unfortunately, the ability to differentiate between basement structures and very local basement lithology changes is limited. An unknown but probably small percentage of mapped basement structures will fail to shoot out on seismic profiles.

Gravity and seismic data will help to confirm some prospects and to cull others. Integration of all geological and geophysical information sources will help to better understand the aeromagnetic signatures. Any prospects pursued in the study area should be approached from a multiple pay approach. Paleozoic targets are riskier than Cretaceous ones due to the limited drilling information, but the potential reward is very attractive. If feasible, wells should be taken to Precambrian to test possible deeper Pennsylvanian and granite wash potential. It is very likely that future drilling will be able to locate new reservoirs and hydrocarbon sources in this major regional Paleozoic basin shelf.

REFERENCES CITED

Allingham, J.W. and I. Zietz, 1962. Geophysical data on the Climax Stock, Nevada Test Site, Nye County, Nevada: Geophysics, vol. 27, p. 599.

Baars, D.L. and G.M. Stevenson, 1981. Tectonic evolution of the Paradox Basin, Utah and Colorado, *in* D.L.Wiegend, ed., Geology of the Paradox Basin: RMAG Field Conference Guidebook, pp. 23-31.

Baars, D.L., et al., 1988. Basins of the Rocky Mountain region, *in* Sloss, L.L., ed., Sedimentary cover--North American Craton; U.S.: Boulder, CO, Geological Society of America, The Geology of North America, v. D-2., pp. 109-220.

Blakely, R.J., 1995. Potential Theory in Gravity and Magnetic Applications. Cambridge: Press Syndicate of the University of Cambridge, 441 p.

Caudill, Maureen, 1987. Neural network primer, part 1, *in* AI Expert, December, 1987, pp. 46-52.

Cohn, D.A., Z. Ghahramani, and M.I. Jordan, 1995. Active learning with statistical models, *in* G. Tesauro, D. Touretzky, and T. Leen, eds., Advances in Neural Information Processing Systems 7, Cambridge: MIT Press, pp. 705-712

Cordell, L. and V.J.S. Grauch, 1985. Mapping basement magnetization zones from aeromagnetic data in the San Juan basin, New Mexico, *in* W.J. Hinze, ed., The Utility of Regional Gravity and Magnetic Anomaly Maps, pp. 181-197.

Currie, R.G., C.S. Grommé, and J. Verhoogen, 1963. Remanent magnetization of some upper Cretaceous granitic plutons in the Sierra Nevada, California: Journal of Geophysical Research, vol. 68, p. 2263.

DeVoto, Richard H., 1980. Pennsylvanian stratigraphy and history of Colorado, *in* Colorado Geology: RMAG Field Conference Guidebook, pp.71-102.

Dobrin, Milton and Carl Savit, 1988. Introduction to Geophysical Prospecting. New York:

McGraw-Hill, Inc., 867 p.

Efron, Bradley and R.J. Tibshirani, 1993. An Introduction to the Bootstrap. New York: Chapman and Hall, 436 p.

Edwards, Jonathon, Jr., 1963. Petrography of the basement rocks beneath the Denver Basin in Colorado, *in* Geology of the Northern Denver Basin and Adjacent Uplifts: RMAG Field Conference Guidebook, pp.208-210.

Guo, Yi, 1992. Feature Recognition from Potential Fields Using Neural Networks. M.S. Thesis T-4194, Colorado School of Mines, 75 p.

Hart, Don, 1992. Independents harvest Nebraska's Paleozoic zones, *in* Western Oil World, Vol. 49, No. 11, pp. 46-50.

Hawes, J., 1952. A magnetic study of the Spavinaw granite area, Oklahoma: Geophysics, vol. 17, p. 27.

Hertz, J.A., R.G. Palmer, and A.S. Krough, 1991. Introduction to the theory of neural computation. Redwood City, CA: Addison-Wesley Publishing Co., 327 p.

Hinze, William J. and I. Zietz, 1985. The composite magnetic-anomaly map of the conterminous United States, *in* W.J. Hinze, ed., The Utility of Regional Gravity and Magnetic Anomaly Maps, pp. 1-24.

Hoyt, John H., 1963. Permo-Pennsylvanian correlations and isopach studies in the northern Denver Basin, *in* Geology of the Northern Denver Basin and Adjacent Uplifts: RMAG Field Conference Guidebook, pp. 68-83.

Larson, E.E., T.R. Walker, P.E. Patterson, R.P. Hoblitt, and J.G. Rosenbaum, 1982. Paleomagnetism of the Moenkopi Formation, Colorado Plateau: basis for long-term model of acquisition of chemical remanent magnetism in red beds, *in* Journal of Geophysical Research, Vol. 87, pp. 1081-1106.

Lidiak, Edward G., 1972. Precambrian Rocks in the Subsurface of Nebraska. University of Nebraska Conservation and Survey Division, Lincoln, 41p.

Love, J.D. and Ann Coe Christiansen, 1985. Geologic Map of Wyoming. United States Department of the Interior, Reston, 3 sheets, Map #GSG0050-1-2.

Moll, R.F., W.C. Pearson, J.R. Rogers, J.M. Wiener, 1994. United States Patent #5,355,313. Neural network interpretation of aeromagnetic data, 21 claims, 4 drawing sheets.

Momper, James A., 1966. Stratigraphic principles applied to the study of the Permian and Pennsylvanian systems in the Denver Basin, *in* Wyoming Geological Association Twentieth Annual Conference, pp. 87-90.

Montgomery, S. (ed.), 1987. Western Nebraska: The Late Paleozoic Comes of Age, Vol. 4, No. 1, Petroleum Information Corp., 74 p.

Nelson, M.M. and W.T. Illingworth, 1991. A Practical Guide to Neural Nets. Reading, MA: Addison-Wesley Publishing Co., 344 p.

Nettleton, L.L., 1976. Gravity and Magnetics in Oil Prospecting, 2nd edition. New York: McGraw-Hill, Inc., 464 p.

NeuralWare, Inc., 1990. Neural Computing: NeuralWorks Professional II/PLUS and Neural Works Explorer. Pittsburgh: NeuralWare, Inc. Technical Publications Group, 354 p.

Pearson, W.C., J. Wiener, and R.F. Moll, 1990. Aeromagnetic structural interpretation using neural networks: a case study from the northern Denver-Julesburg Basin, *in* Expanded Abstracts of the Technical Program, SEG Sixtieth Annual Meeting, pp. 587-590.

Rogers, James and Mark W. Longman, 1988. Pennsylvanian carbonate facies and porosity types in Bird and Amazon Fields, Cheyenne County, Nebraska, *in* S.M. Goolsby and M.W. Longman, eds., Occurrence and Petrophysical Properties of Carbonate Reservoirs in the Rocky Mountain Region: RMAG Field Conference Guidebook, pp. 23-35.

Rogers, Samuel J., J.H. Fang, C.L. Karr, and D.A. Stanley, 1992. Determination of lithology from well logs using a neural network, *in* American Association of Petroleum Geologists Bulletin, Vol. 76, No. 5, pp. 731-739.

Ross, R.J. and Ogden Tweto, 1980. Lower Paleozoic sediments and tectonics in Colorado, *in* Colorado Geology: RMAG Field Conference Guidebook, pp. 23-35.

Rumelhart, D.E. and James L. McClelland, 1986. Parallel Distributed Processing: Explorations in the Microstructure of Cognition, Volume 1. Cambridge: Massachusetts Institute of Technology Press, 546 p.

Sahl, H.L., F.I. Pritchett, Jr., and P.T. Loeffler, 1993. Kleinholz Paleozoic field study, Kimball County, Nebraska, *in* The Mountain Geologist, Vol. 30, No. 3, pp 81-94.

Sonnenberg, Stephen A. and Robert J. Weimer, 1981. Tectonics, Sedimentation, and Petroleum, Northern Denver Basin, Colorado, Wyoming, and Nebraska: Colorado School of Mines Quarterly, Vol. 76, No. 2., 45 p.

Specht, Donald, 1990. Probabilistic neural networks, *in* Neural Networks, vol. 3, pp. 109-118.

Telford, W.M., L.P. Geldart, and R.E. Sheriff, 1990. Applied Geophysics. Cambridge: Cambridge University Press, 770 p.

Tweto, Ogden, 1980a. Tectonic history of Colorado, *in* Colorado Geology: RMAG Field Conference Guidebook, pp. 5-20.

Tweto, Ogden, 1980b. Precambrian geology of Colorado, *in* Colorado Geology: RMAG Field Conference Guidebook, pp. 37-46.

Vacquier, V., Nelson Clarence Steenland, Roland G. Henderson, and Isidore Ziets, 1963. Interpretation of Aeromagnetic Maps. GSA Memoir 47. New York: New York Lithographing Corp., 151 p.

Warner, L.A., 1980. The Colorado Lineament, *in* Colorado Geology: RMAG Field Conference Guidebook, pp. 11-21.

Watney, W.L., 1980. Cyclic sedimentation of the Lansing-Kansas City Groups in northwestern Kansas and southwestern Nebraska: Kansas Geological Survey Bulletin 220, 72p.

Webring, M., 1981. MINC: A gridding program based upon minimum curvature. U.S. Geological Survey Open File Report 81-1224, 41 p.

Weimer, Robert J., 1980. Recurrent movement on basement faults, a tectonic style for Colorado and adjacent areas, *in* Colorado Geology: RMAG Field Conference Guidebook, pp. 23-35.

Weiss, S.M. and I. Kapouleas, 1989. An empirical comparison of pattern recognition, neural nets, and machine learning classification methods, *in* Proceedings of the International

Joint Conference on Artificial Intelligence, pp. 781-787.

Weiss, S.M. and C.A. Kulikowski, 1991. Computer Systems that Learn. Morgan Kaufmann, 1991, 223 p.